Cement and Concrete Composites 104 (2019) 103389

Contents lists available at ScienceDirect

Cement and Concrete Composites

journal homepage: www.elsevier.com/locate/cemconcomp

Impact resistance of fiber-reinforced concrete – A review

Doo-Yeol Yoo[a,*], Nemkumar Banthia[b]

[a] Department of Architectural Engineering, Hanyang University, 222 Wangsimni-ro, Seongdong-gu, Seoul, 04763, Republic of Korea
[b] Department of Civil Engineering, The University of British Columbia, 6250 Applied Science Lane, Vancouver, BC, V6T 1Z4, Canada

ARTICLE INFO

Keywords:
Fiber-reinforced concrete
Impact resistance
Strain rate
Fiber type
Strength enhancement
Supplementary cementitious material

ABSTRACT

This paper reviews the state of the art of the impact resistance of ordinary fiber-reinforced concretes (FRCs) containing various fibers. First, various types of impact test methods that are current available are addressed as well as some concerns about them based on extensive literature reviews and our perspective. Then, common properties of FRCs under impact loading regardless of fiber type, such as the reasons for their enhanced strength under impact, the effect of size on impact resistance, and several factors (i.e., matrix strength, loading conditions, and fiber existence) that influence strain-rate sensitivity, are discussed. Furthermore, the comprehensive impact resistances of FRCs with various fibers (i.e., steel, polymeric, carbon, basalt, natural, and hybrid fibers) are investigated under different loading conditions. After summarizing the impact properties of FRCs with various fibers, the comparative impact resistance of FRCs according to the fiber type is evaluated to determine which type gives the best improvement of impact resistance. Lastly, the effect of supplementary cementitious materials (SCMs), i.e., fly ash, silica fume, and slag, on the impact resistance of FRCs is examined, and some combinations of SCM and fiber types that lead to enhanced impact resistance are suggested.

1. Introduction

Concrete has been widely used as a construction material in combination with deformed steel reinforcing bar (rebar) and prestressing strand. Since they have great compressive strength, the steel rebar or strands are only adopted in zones in which tensile or shear stress occur, which have been called reinforced concrete (RC) or prestressed concrete (PSC) elements. The enhanced tensile or shear resistance of RC and PSC leads to their successful use as structural elements under quasi-static loading conditions. However, in recent years, civil structures or buildings have frequently been exposed to extreme loading conditions, such as impacts, blasts, and fire from a variety of sources, including terrorist attacks. Although ordinary RC and PSC structures are successfully used under static conditions, they are insufficient under extreme loads because of the poor energy absorption capacity and brittle nature of concrete, which lead to its fragmentation. To overcome the drawbacks of plain concrete under impacts and blasts, researchers [1–3] have suggested concrete strengthened with continuous textiles, discontinuous short fibers, external fiber-reinforced polymer, etc. Among others, the inclusion of discontinuous fibers made of materials such as steel, polymer, carbon, and basalt, has been most widely adopted by researchers because of its several advantages: (1) they are easy to include in concrete mixtures, (2) they are effective in enhancing concrete's toughness under impact or blast by fiber bridging, and (3) they are more cost effective than other methods.

Concrete that contains discontinuous fibers with random orientation is called fiber-reinforced concrete (FRC). The randomly orientated fibers can effectively resist crack propagation and widening in the cement matrix, improving the post-cracking ductility of concrete under both static and impact loads. The fibers' effectiveness in enhancing post-cracking ductility depends on their bond performance, which is affected by factors such as the number of fibers per unit area, fiber orientation, fiber shape and aspect ratio, matrix strength, etc. Thus, to properly design FRC for practical application to civil structures and buildings, the factors affecting post-cracking ductility must be comprehensively investigated. The comprehensive mechanical properties and developments of FRCs including various fiber types (i.e., steel, glass, synthetic, and carbon fibers) in static conditions were reviewed by Brandt [4]. If the properties of FRCs are independent of the loading rate, the previous review paper [4] can provide useful information to researchers and engineers who are interested in using FRCs for protective structures under extreme loads. However, unfortunately, plain concrete and FRCs are both very sensitive to loading rates (i.e., strain or stress rates), exhibiting totally different behaviors under impact as compared to static conditions, thus requiring a new review of the state of the art on the impact resistance of FRC. In this paper, several

* Corresponding author.
E-mail addresses: dyyoo@hanyang.ac.kr (D.-Y. Yoo), banthia@civil.ubc.ca (N. Banthia).

https://doi.org/10.1016/j.cemconcomp.2019.103389
Received 9 November 2018; Received in revised form 12 June 2019; Accepted 6 August 2019
Available online 07 August 2019
0958-9465/

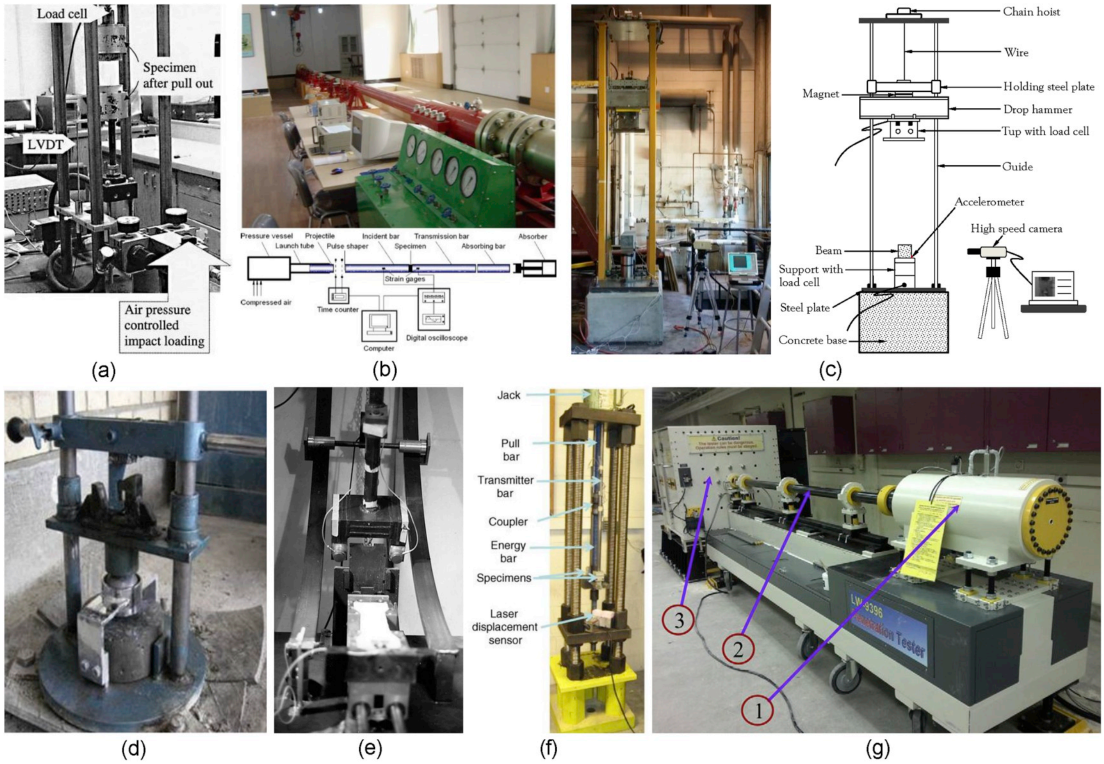

Fig. 1. Various impact test machines; (a) fiber pullout impact test [6], (b) SHPB test [13], (c) drop-weight impact test [18], (d) free falling ball test [19], (e) charpy impact test [21], (f) strain energy impact test system [5], (g) air-gun impact test (1. power unit, 2. guide barrel, and 3. target frame and test section) [24].

important points regarding the impact resistance of FRCs are addressed as follows: (1) a summary of current impact testing methods; (2) some limitations and solutions of current impact testing methods; (3) the general impact behaviors of FRCs regardless of fiber type, (4) the specific impact response of FRCs by fiber type, i.e., steel, polymer, carbon, basalt, and natural sources; and (5) the comparative impact resistances of FRCs by fiber type, which suggests the best ones for use in protective structures. Finally, we examine the effect of supplementary cementitious materials (SCMs), which are now widely used in eco-friendly concrete mixtures, on the impact resistance of FRCs.

2. Impact test machines and methods

2.1. Types of impact test methods

Several types of impact test methods are available worldwide, as shown in Fig. 1. Kim et al. [5] categorized the high strain-rate test methods into four classes: (1) methods based on potential energy, in which a large mass freefalls onto the specimens (i.e., the drop-weight impact, Charpy, and Izod tests); (2) methods based on kinetic energy, in which a mass strikes the specimen very rapidly (i.e., the gas gun and fiber pullout impact tests); (3) methods in which hydraulic machines deform specimens at a medium loading rate; and (4) methods based on stress wave propagation, in which a stress wave is generated and propagated through a long steel bar and impacts the specimens (i.e., the split Hopkinson pressure bar (SHPB) test). Given the loading condition (compression, tension, flexure, or projectile) and type of specimen (e.g., cylinder, cube, beam, or slab), engineers can adopt the proper impact test methods. In this section, some of the impact test methods most widely used, mentioned above, are summarized and discussed.

- *Fiber pullout impact test*: The fiber pullout impact test utilizes kinetic energy from air or a nitrogen gas gun [6–8]. The test setup is given in Fig. 1a. A single fiber is embedded in a preseparated specimen; the top half is fixed to the machine, whereas the bottom half is pulled down at a high speed using air pressure. The load cell is installed at the top of the machine to measure the impact pullout load, and a laser linear differential displacement transformer (LVDT) measures the slip of the fiber from the cement matrix. Depending on the magnitude of the air and nitrogen gun pressure, very high pullout displacement rates can be achieved. According to the test machines installed, the maximum loading rates are different: for example, the maximum pullout loading rates, reported by Bindiganavile and Banthia [6], Tai et al. [7], and Yoo and Kim [8], were about 3000 mm/s, 1800 mm/s, and 1700 mm/s. The fiber pullout impact machine adopted by Yoo and Kim [8] can achieve the maximum pullout loading rate of about 4800 mm/s without specimens. If it is assumed to adopt a gauge length of 80 mm for composite tensile specimen in accordance with the JSCE recommendations [9], the maximum strain-rates are able to be from approximately 21.3/s to 37.5/s, respectively. These rates can be included in the range of hard impact and explosive blast loads [10,11], as shown in Fig. 2.
- *SHPB test*: This test method is frequently adopted by researchers to evaluate the dynamic compressive and splitting tensile behaviors of concrete [12–14]. This test is based on two basic assumptions: (1) one-dimensional stress pulse propagation and (2) stress uniformity along the specimen thickness. As shown in Fig. 1b, the SHPB test includes several solid circular steel bars, which are aligned in the direction of a specimen, and a specimen sandwiched between two long bars. The diameter and length of the incident, transmission, and absorbing steel bars differ with researchers' objectives. A projectile strikes the incident bar, and the resulting incident stress pulse propagates along the bar to the interface between the incident bar and specimen, where it is reflected or transmitted. The stress wave reflection is obtained at the interface between the specimen and steel bar to homogenize the stress distribution in the specimen [15]. The transmitted stress pulse propagates through the specimen into the absorbing bar. The stress, strain, and strain-rate of the specimen can be calculated from the forces used, which are obtained from

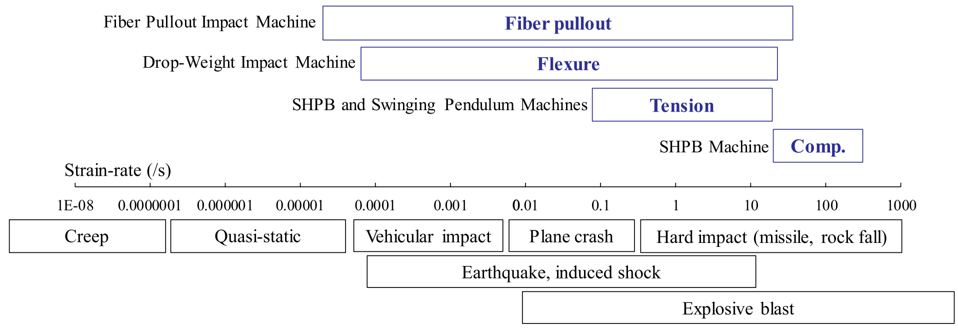

Fig. 2. Typical strain-rate ranges for concrete structures [10,11] and summary of available strain-rate ranges for all loading conditions based on literature reviews.

attached strain gauges at both the transmission and absorbing bars, and the particle velocities at the interfaces between the incident and transmission bars and the specimen.

- *Drop-weight impact test*: This test method is based on potential energy. A heavy hammer freefalls from a height, striking the specimen, to evaluate the specimen's flexural and compressive behaviors [16,17]. As shown in Fig. 1c, an impact load is applied to the middle of the specimen by dropping a mass from a drop height, leading to a certain potential energy. The impact velocity can be simply calculated by assuming that there is no friction between the guide and hammer using the following equation: $E_P = 1/2mv^2$, where E_p is potential energy, m is the hammer's mass, and v is velocity. Since the impact load—measured from a load cell affixed to the drop hammer—includes inertial load, two methods for measuring actual impact load can be applied: (1) measuring the reaction load from supports [18] and (2) substituting the inertial load from the measured impact load based on the specimen's acceleration [17]. To obtain a load–deflection curve, a potentiometer, laser LVDT, and accelerometer are used to measure midspan deflection.
- *Free falling ball test*: This is a potential-energy-based impact test method [19] recommended by the American Concrete Institute (ACI) Committee 544 for measuring the impact resistance of FRC. As illustrated in Fig. 1d, a round steel ball is dropped from a height to cylindrical samples with a diameter of 150 mm and a height of 64 mm. The number of blows required to cause an initial crack and sample failure is recorded; specimens with more blows at first crack and failure have higher impact resistance. The energy absorption capacity of the sample is calculated by multiplying the potential energy and number of blows.
- *Charpy impact test*: This test method is similar in principle to the drop-weight impact testthat it is based on the potential energy of a heavy mass [20,21] and can be applied to both tensile and fiber pullout tests, as shown in Fig. 1e. A swinging pendulum hits a specimen in its pathway, and momentum is transferred to the specimen, causing a high strain rate. A notched specimen is gripped with a frame: one support (A) is fixed, whereas the other support (B) is placed on rollers. The swinging pendulum impacts the support (B), causing an impact force on the specimen. The load is measured from a load cell affixed to the fixed support (A). Load–displacement curves under impact are obtained by measuring the displacement of the support (B).
- *Strain energy impact test system (SEITS)*: As shown in Fig. 1f, this test setup provides high strain-rate kinetic energy to specimens via the sudden release of stored strain energy in a long steel bar [5]. First, load is continuously applied to a short bar, which is connected with a long energy bar by a coupler. Once the applied load exceeds the coupler strength, a sudden, brittle failure occurs in the coupler and the stored energy in the long energy bar is abruptly released. If the energy bar is perfectly attached to the specimen, the stress wave is directly applied to the specimen, as in the mechanism of SHPB, and if there is a gap between the energy bar and specimen, both the stress wave and kinetic energy are applied to the specimen. Several impact test machines based on the SEITS, such as the strain energy frame impact machine (SEFIM) and modified SEFIM, have been also suggested [22,23].
- *Projectile impact test*: This impact test method is based on kinetic energy. As shown in Fig. 1g [24], a projectile is launched via air or gas gun. Several projectile nose shapes (e.g., conical, biconical, ogive, and flat) are available; impact performance can differ depending on this shape. The projectile impact test quantitatively evaluates impact resistance using local damage to the concrete plate or slab—including the diameters of the front and rear faces' craters, penetration depth, residual velocity of the projectile, and weight loss.

2.2. Concerns regarding current impact test methods

Fig. 2 shows typical strain-rate ranges for concrete structures [10,11] and summarizes the available strain-rate ranges for all loading conditions, i.e., compression, tension, flexure, and fiber pullout, based on extensive literature reviews. For the compressive tests, SHPB machine has been mainly adopted and most of available test data on the dynamic compressive behavior of FRCs are included in the hard impact and explosive blast loading rates, faster than other loading conditions. Although smaller strain-rate was applied for the dynamic tensile tests based on the SHPB and swinging pendulum machines than the compression, it was included in more various kinds of dynamic loads, i.e., the plane crash, earthquake, induced shock, hard impact, and explosive blast. The strain-rate ranges adopted by researchers for dynamic flexural and fiber pullout tests were quite similar, as shown in Fig. 2, but they were wider than those of dynamic tensile and compressive tests. Therefore, they can be included in more various kinds of dynamic loads, such as vehicular impact, plane crash, earthquake, induced shock, hard impact, and explosive blast. The available strain-rate ranges, dynamic increase factors (DIFs), and some other useful findings of FRCs are summarized in Table 1.

Bentur et al. [17] reported that specimen (beam or plate) inertia plays a substantial role in drop-weight impact load because of its high loading rate. In general, the impact load—measured from a load cell affixed to a drop hammer—increases very steeply immediately after impact, while almost no reaction load or deflection were measured during this period [25]. This means that a large portion of the initial impact load, which is obtained from the hammer load cell, is caused by the inertial force exerted on the beam opposite to the acceleration direction [17]. Therefore, to obtain the actual impact load that causes specimen failure, the inertial load must be excluded from the impact load measured from the hammer. Banthia et al. [26] have suggested a method to exclude the inertial load from the measured impact load based on the measured acceleration and virtual work expression. By assuming a linear acceleration distribution along the beam length, the inertial load can be calculated based on the sample's geometry, density, and midspan acceleration. Other researchers [18,27–29] have

Table 1
Summary of some findings from various impact tests.

Author	Type of testing machine	Loading condition (Spec. type)	Comp. strength [MPa]	Type of fiber	Fiber geometry [l_f/d_f, mm/mm]	Fiber volume fraction [%]	Loading rate	Strain-rate [/s]	DIF	Summary of results
Yoo et al. [2]	Drop-weight impact machine	Flexure (Beam)	90.1–96.5	Hooked steel fiber	30/0.5	0–2	-	3.37–4.76	1.49–1.75	Both the static and impact resistance of SFRC are improved by increasing fiber volume fraction. But, the loading rate sensitivity decreased with increasing the fiber volume fraction.
Bindiganavile and Banthia [6]	Fiber pullout impact machine	Pullout (Dog-bone/aligned)	40	Straight PO fiber	50/-	Single	2,000, 3000 mm/s	25, 37.5[b]	5.17, 7.07	Pullout resistance of both polymeric and steel fibers generally increased with increasing the loading rate. Steel fiber showed poorer pullout resistance, in terms of bond strength and energy aborption capacity, than the polymeric fibers at very high loading rates.
				Sin. crimped PP fiber[a]	30/-				3.57, 3.64–3.80	
				Sin. crimped PP fiber	50/-				1.90, 2.84	
				Flat-end steel fiber	30/0.73				2.61, 1.92	
Lok and Zhao [12]	SHPB	Compression (Cylinder)	90	Hooked steel fiber	35/0.54	0.6	-	19.8–103	1.02–1.75	Compressive strength of SFRC increased with increasing the strain-rate, similar to the plain concrete. Post-peak ductility of SFRC under compression becomes absent at the strain-rate exceeding 50/s, meaning that the compressive ductility of SFRC is able to be achieved only at low strain-rate.
Banthia et al. [64]	Drop-weight impact machine	Flexure (Beam)	54–55	Hooked steel fiber	30–35/0.5–0.55	0.77	28,830 MPa/s	0.71	5.06–7.28	Adding steel and synthetic fibers was highly effective in enhancing the fracture energy absorption and toughness under impact. Steel fibers provided the greatest improvement in toughness under both static and impact loading. PP and PVA fibers enhanced the toughness reasonably, but carbon fiber failed to provide any improvement.
			51	Flat-end steel fiber	30/0.73	0.77			6.70	
			45–49	Straight PP fiber	25–38/0.38–0.76	1–1.5			7.15–8.67	
			50–52	Straight carbon fiber	10–18/0.017–0.018	2			7.02–12.45	
			50	Flat-end PVA fiber	30/0.55 × 0.75[c]	0.77			7.86	
			53	Twin-coned steel fiber	35/1	0.77			4.60	
Banthia et al. [20]	Swinging pendulum machine	Tension (Dog-bone)	75–85	Carbon fiber	3/0.018	1–3	8000 MPa/s	0.4	1.08–1.53	Cement paste and mortar became stronger and tougher under impact and these improvements were greater at higher fiber volume fractions. The order of strain-rate sensitivity on the tensile strength was as follows: PP fiber > steel fiber > carbon fiber.
				Flat-end steel fiber	3/0.005 × 0.025				1.13–1.99	
				Straight PP fiber	6/0.004				1.04–2.12	
Banthia et al. [21]	Swinging pendulum machine	Tension (Dog-bone)	43–90	Hooked steel fiber	60/0.8	0.5	3500 MPa/s	0.08	1.17–1.41	Fiber reinforcement was effective in improving fracture energy absorption capacity under impact. Strength of matrix has a decisive effect: the higher strength of matrix led to the less effectiveness on the steel fibers in enhancing the fracture energy absorption under impact.
			40–84	Crimped steel fiber	60/1.0				1.10–1.14	
			43–83	Crimped steel fiber	52/2.3 × 0.55				1.28–1.32	
			38–86	Twin-coned steel fiber	62/1.0				1.21–1.64	

(*continued on next page*)

Table 1 (*continued*)

Author	Type of testing machine	Loading condition (Spec. type)	Comp. strength [MPa]	Type of fiber	Fiber geometry [l_f/d_f, mm/mm]	Fiber volume fraction [%]	Loading rate	Strain-rate [/s]	DIF	Summary of results
Zhang et al. [27]	Drop-weight impact machine	Flexure (Beam)	92	Hooked steel fiber	50/0.75	0.82	0.1–2660 mm/s	-	1.12–3.48	Dynamic increase factors on the peak load and fracture energy of SFRCs were approximately 3.5 and 2.5, respectively, for the highest impact velocity at 2660 mm/s.
Yoo et al. [30]	Drop-weight impact machine	Flexure (Beam)	39–191	Hooked steel fiber	30/0.5	0.5–2	23,006–123,249 MPa/s	3.29–11.45	1.53–5.20	Post-peak behavior was improved with fiber content. Increases of fiber content and strength led to the enhancement in residual flexural performance. At higher strength, less sensitivity to the strain-rate was obtained under flexure.
Dey et al. [31]	Drop-weight impact machine	Flexure (Beam)	5.61	Straight PP fiber	12/0.048	0.5	-	0.02–22.4	2.32–4.82	Impact resistance of masonry structure can be improved by adding PP fibers. FRAC showed more than three times higher flexural toughness than AAC due to the role of short fibers in bridging the flexural cracks and absorbing the impact energy.
Bindiganavile and Banthia [32]	Drop-weight impact machine	Flexure (Beam)	38	Straight PO fiber	50/-	0.75	13,300 MPa/s	0.33	2.62	Flexural strength of FRC increased at impact.
			40	Sin. crimped PP fiber[a]	30/-		15,500 MPa/s	0.38	2.34	Toughness of FRC with polymeric fibers was enhanced under impact, whereas that of SFRC was rather reduced.
			43	Sin. crimped PP fiber[a]	50/-		16,100 MPa/s	0.40	2.33	Effectiveness of polymeric fibers
			43	Flat-end steel fiber	30/0.73		12,900 MPa/s	0.32	1.52	increased under impact, whereas that of steel fibers rather decreased.
Gokoz and Naaman [55]	Fiber pullout impact machine	Pullout (Dog-bone/aligned)	-	Straight steel fiber	38/0.4	Single	500–2000 mm/s	6.25–25	1.44–2.70	PP fiber gave most rate sensitivity on the tensile strength than steel and glass
				Straight PP fiber	-/0.38				2.25–7.43	fibers. PP fiber exhibited the highest energy
				Glass fiber	38/0.0715				1.03–2.39	absorption capacity at high loading rates (impact), followed by the steel fiber and glass fiber.
Pacios et al. [58]	Charpy pendulum test machine	Pullout (Dog-bone/aligned)	57.78	Straight steel fiber	12.7/0.4	Single, multiple	1.70×10^{-3}–528.47 mm/s	2.11×10^{-5}–6.61	0.78–10.50	Maximum pullout load and slip capacity of multiple steel fibers in ordinary cement matrix increased with the loading rate. Increasing the number of fibers was effective in increasing the rate sensitivity but ineffective on the average bond strength.
Banthia and Trottier [59]	Charpy impact test machine	Pullout (Dog-bone/aligned)	-	Hooked steel fiber	60/0.6	Single	1.5 mm/s	0.019	1.39–4.59	At the identical failure mode, pullout energy of deformed steel fibers
				Crimped steel fiber	58/1.0				0.93–2.26	increased under impact loads. Hooked steel fiber has higher rate
				Crimped steel fiber (half circular)	53/0.5 × 2.2				0.87–1.81	sensitivity than the crimped steel fiber.

(*continued on next page*)

Table 1 (*continued*)

Author	Type of testing machine	Loading condition (Spec. type)	Comp. strength [MPa]	Type of fiber	Fiber geometry [l_f/d_f, mm/mm]	Fiber volume fraction [%]	Loading rate	Strain-rate [/s]	DIF	Summary of results
Gupta et al. [65]	Drop-weight impact machine	Flexure (Plate)	54–55	Hooked end steel fiber	30–35/0.5–0.55	0.77	1046 MN/s	1.08	1.53–1.60	Wet-mix shotcrete with various fibers was highly sensitive to the loading rate: stronger, stiffer, and tougher at impact. The ability of an efficient fiber to reinforce concrete is magnified and clearly visible in plates than in beams. FRCs with polymeric fibers exhibited higher rate sensitivity on the flexural strength than SFRCs.
			51	Flat-end steel fiber	30/0.73	0.77			1.32	
			45–49	Straight PP fiber	25–38/0.38–0.63	1–1.5			2.56–3.30	
			48	Crimped PP fiber	30/0.76	1.5			3.58	
			50–52	Straight carbon fiber	10–18/0.017–0.018	2			1.61–4.51	
			54	Flat-end PVA fiber	30/0.55 × 0.75	0.77			2.49	
			53	Twin-coned steel fiber	35/1.0	0.77			2.69	
Hao and Hao [71]	SHPB	Splitting Tension (Cylinder)	-	Spiral steel fiber	15/0.56	0–1.5	about 150,000 MPa/s	about 2–20	2.5–6.7	Adding steel fibers and increasing their volume fraction led to higher rate sensitivity on the splitting tensile strength of concrete.
Wang et al. [74]	SHPB	Compression (Cylinder)	81.8–90.7	Straight steel fiber	13/0.16	0.5	-	100–300	1.6–1.7	Lower rate sensitivity on the compressive strength and elastic modulus of HSC was observed by adding fibers.
				Straight PE fiber	12/0.039	0.5			1.8–2.1	Using 0.5% steel fiber was recommended for enhancing impact resistance of HSC than the PE fiber or hybrid of them.
				Steel and PE fiber hybrid	-	1.0			1.7–2.2	
Yet et al. [78]	SHPB	Compression (Cylinder)	51.03–74.38	Hooked steel fiber	35/0.55	0–1.5	-	30.21–64.63	1.61–2.62	Adding steel fiber was effective in improving static and dynamic compressive strengths.
de Andrade Silva et al. [111]	Drop-weight impact machine	Flexure (Beam)	70	Sisal fiber	-/0.04–0.05	10	-	3.8–5.8	0.76–0.96	There was no strain-rate effect on the flexural strength of concrete with sisal fibers.
Suaris and Shah [121]	Drop-weight impact machine	Flexure (Beam)	57.6 45.9 57.6 50.3	Steel fiber Steel fiber PP fiber Glass fiber	25.4/0.25 6.4/0.15 63.5/0.20 25.4/-	1.0	-	6.8×10^{-5}–0.27	1.15–1.92 1.17–1.90 1.09–1.69 1.02–2.00	Steel and glass FRCs were more sensitive to strain-rate than the mortar itself, while the PP FRC shows similar rate sensitivity with the mortar itself. Matrix cracking in FRC is a major process responsible for strain-rate sensitivity.

[Note] DIF = dynamic increase factor, PO = polyolefin, PP = polypropylene, SFRC = steel fiber-reinforced concrete, FRC = fiber-reinforced concrete, FRAC = fiber-reinforced aerated concrete, AAC = autoclaved aerated concrete, PE = polyethylene, and HSC = high-strength concrete.

[a] Sinusoidally crimped PP fiber.

[b] Strain-rate is calculated by assuming the gauge length of 80 mm based on JSCE recommendations [9].

[c] Cross-sectional dimension of fiber.

measured the pure load, excluding the inertial term, using support load cells. Since the reaction load measured from support load cells does not include inertial force, it can be directly adopted for obtaining strengths and load–displacement curves. However, Yoo et al. [29] recently pointed out that RC beams with higher span-to-depth ratios exhibit unrealistic reaction load versus midspan deflection curves under drop-weight impact, mainly because the slow stress wave in concrete causes a delayed increase in the reaction load.

Yoo et al. [30] compared the reaction load versus midspan deflection histories of concrete beams with a cross-section of 100 mm × 100 mm and a length of 400 mm under drop-weight impact loads. The midspan deflections were obtained from a potentiometer and an accelerometer. Their interesting findings showed that the load–deflection curves displayed different behaviors with each measurement device. Since the beams completely failed very quickly (1 m s), an unrealistic load–deflection curve was obtained from the potentiometer. On the contrary, the deflection, which was calculated from double integration of the acceleration measured from accelerometer, started to increase at the same time as the reaction load. Therefore, a reasonable reaction load–deflection curve was obtained. Thus, previous researchers [25,31] have adopted the accelerometer to calculate the midspan deflection of small-sized concrete beams under impact loads.

The correlation between single-aligned fiber pullout resistance and beam tests under impact loads was examined by Bindiganavile and Banthia [6,32]. They reported a lack of agreement between these test methods for the following reasons. First, the effect of fiber orientation could not be considered in the single-fiber pullout test, even though most fibers in the beam are randomly oriented. Second, fiber-fiber interaction remains obscured in the single-fiber pullout test. Lastly, the actual crack opening rate in the beam under drop-weight impact was not identical to the loading rate applied to the single-fiber pullout test. Therefore, further study is required to resolve the disagreement between the single fiber pullout-test and beam test under impact loads.

Based on several decades of study on the impact resistance of FRC, Banthia [33] has insisted that it is very difficult to standardize impact test methods for FRC because data reported in the literature cannot be compared. These data were obtained from different impact machines using various support systems, different mechanisms of energy loss, and different methods for providing a high loading rate, greatly influencing the test results. As can be seen in Fig. 3 [33], considerably different flexural toughness values were obtained from identical FRC materials using impact test machines with different capacities. Thus, data comparison is only possible when results are obtained from machines with similar capacities.

3. Common properties of FRC under impact

The strength of FRC is sensitive to the rate of loading [34], mainly because (1) crack growth resistance is enhanced (greater stress intensity factor K_I) with increasing crack velocity under impact [35] and (2) the crack path is altered and shortened with increasing loading rate because crack propagation is significantly slower than applied stress [36]. Increased crack velocity was successfully observed from Bindiganavile and Banthia [35] using a contoured double-cantilever beam test under drop-weight impact loads, while the shortened crack path under impact was experimentally observed by Tai et al. [7] based on a scanning electron microscope (SEM) study, as shown in Fig. 4.

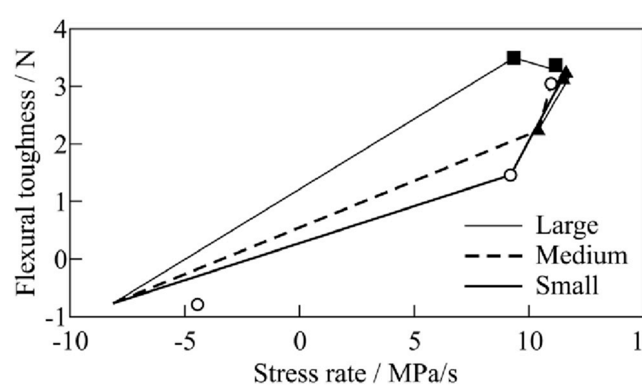

Fig. 3. Influence of machine capacity on measured impact response of a given FRC material [33].

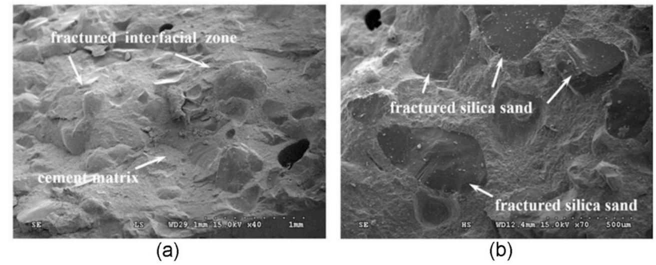

Fig. 4. SEM images for the fractured surface of UHPFRC under various loads; (a) bond fractured extending around aggregate at static load and (b) aggregate fracture at impact load [7].

The strain-rate (or stress-rate) sensitivity of concrete is affected by several factors, such as matrix strength, moisture content, temperature, and loading configurations (compression, tension, and flexure) [32,34,37,38]. Ross [37] noted that tensile strength of ordinary concrete is more sensitive to strain-rate than compressive strength, which is consistent with findings of Banthia et al. [20,39] and Suaris and Shah [38]. They [20,38] further reported that the sensitivity of flexural strength of ordinary concrete to strain rate appears to be an intermediate value between the tensile and compressive strengths, as shown in Fig. 5. Matrix strength also influences the sensitivity of strength to strain or stress rates: Bindiganavile et al. [34], Ross [37], Bentur et al. [40], Banthia [41], and Yoo et al. [25,30] insisted that concrete with a higher strength exhibits less sensitivity to strain- and stress-rates compared to that with a lower strength, whereas Bishoff and Perry [42] reported that higher strength concrete has higher stress-rate sensitivity in compression. The higher strain-rate sensitivity for lower strength concrete might be caused by the significant difference in the strengths of the cement matrix and aggregates. Fully saturated concrete provides increased strain-rate sensitivity compared to dry concrete, as reported by Sercombe et al. [43]. However, there was no obvious effect of subzero temperature on the stress-rate sensitivity of concrete, based on the test results performed by Banthia et al. [44].

To evaluate the size effect on the impact resistance of FRC, it is very

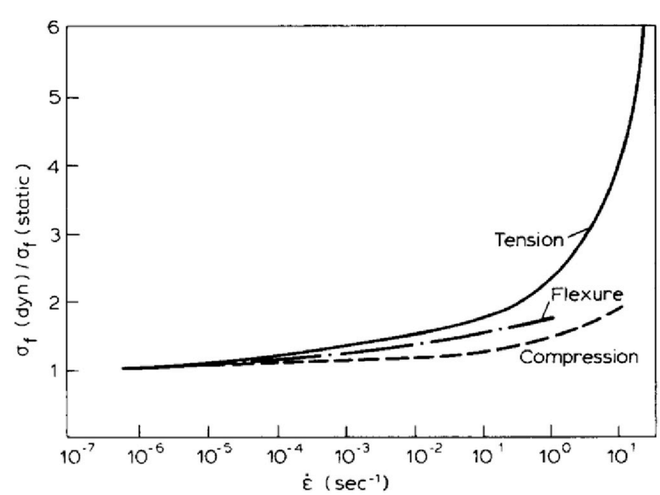

Fig. 5. Relationship between increase in strength and strain-rate of concrete in tension, flexure, and compression [38].

important to ensure that an identical stress- or strain-rate is applied to specimens of various sizes [41]. Qian et al. [45] and Morton [46] also mentioned the importance of maintaining impact velocity to enable scaling. Banthia [41] has examined the effects of specimen size and stress-rate on the impact resistance (including strength and toughness) of FRC beams under drop-weight impacts based on normalized impact data. They reported a clear size effect on the impact toughness of FRCs that include both steel and polypropylene (PP) fibers. The flexural toughness of FRC beams under impacts decreased with increasing specimen size, and the size effect on flexural toughness became more pronounced at higher impact intensities. In addition, the flexural strength of FRC showed a size effect under impact similar to that under static loads, indicating a strength reduction with increasing specimen size.

Wang et al. [47] comprehensively compared the DIF of compressive strength of plain concrete and steel and PP FRC. It was clearly reported that FRC has a smaller DIF for compressive strength as compared with plain concrete at a similar strain-rate, meaning that FRC is less sensitive to loading rate than plain concrete. This is consistent with the findings from Bindiganavile et al. [34]. The lower sensitivity of FRC is based on two reasons. (1) In accordance with ACI Committee 446 [48], concrete strength increases with crack velocity. For the FRC, although higher crack velocity was obtained at higher strain rates, the fibers might slow the crack velocity as compared with plain concrete. In addition, (2) steel fibers may be less sensitive to loading rate compared to concrete, due to its homogeneity and few defects. Thus, the FRCs exhibited lower strain-rate sensitivity than plain concrete.

4. Dynamic crack growth resistance of FRC

In contrast to ordinary concrete, FRC can provide higher closing pressure at crack surface due to fiber bridging effect, acting behind the propagating crack tip where fibers undergo bond-slip process [49] and mitigating the stress intensity factor [50]. The fracture process of FRCs is thus more complex, and a sophisticated model is required to simulate it properly. Previously, cohesive crack model [51] and J-integral [52] were applied to model the fracture behavior of FRC, but these are applicable for only criteria on crack initiation and inappropriate to define its continued crack growth. In order to overcome the limitation of previous approaches, an *R*-curve was adopted by Mobasher et al. [50] for continuously simulating the toughening of cement matrix by fiber reinforcing and monitoring variations of the stress intensity with a crack growth. Banthia et al. [49] reported that the *R*-curve is suitable for evaluating fracture process of FRC at impact if a dynamic stress intensity factor is incorporated, and Bindiganavile and Banthia [35] evaluated the crack growth resistance and effective crack length curve of plain concrete and FRCs with polymeric and steel fibers at various loading rates. They [35,53] reported several useful findings that (1) a higher crack growth resistance is maintained even at larger crack length when the fibers are incorporated; (2) the crack grow resistance increases with increasing the magnitude of input energy and rate of loading; (3) a higher impact rate leads to a faster crack extension; and (4) the existence of fibers decreases the rate of crack growth. Similarly, Mindess et al. [54] observed the crack velocity of plain concrete is only one-tenth (-115 m/s) of the theoretical Rayleigh wave velocity and a further reduction to -75 m/s by adding steel fibers. For the above reasons, a higher fracture toughness is generally obtained under faster loading conditions for the cement-based materials, and FRCs can be effectively applied for protective structures due to their superior and excellent dynamic crack growth resistance.

5. Impact resistance of various types of FRC

FRC exhibits significantly improved impact resistance compared to plain concrete. Due to the fiber bridging effect at crack surfaces, fiber reinforcement is effective in improving the energy absorption capacity of concrete under impact. However, as indicated by Banthia et al. [21], the improvement depends on the fiber type and geometry; as a result, the impact resistance of FRC must be analyzed by fiber type and geometry. This section comprehensively summarizes and analyzes the impact resistance of FRCs including various fiber types.

5.1. Steel fibers

5.1.1. Fiber pullout behavior

Gokoz and Naaman [55] reported that the bond strengths of straight steel, glass, and PP fibers embedded in a Portland cement matrix were only slightly improved at higher loading rates. In particular, they [55] noted that the frictional component of straight steel fiber was almost insensitive to loading rate, which is consistent with findings on the pullout response of smooth steel rebar from Vos and Reinhardt [56] and Naaman [57]. Pacios et al. [58] similarly noted that the overall sensitivity to loading rate was minor for straight steel fibers. Due to the pullout mechanism (only friction) of straight steel fiber, no cracks in the surrounding matrix perpendicular to the interface between the steel fiber and matrix were observed even under high loading rate.

Bindiganavile and Banthia [6] reported that, in general, the bond strength and pullout energy of flat-end steel fibers improved with increasing loading rates, whereas the slip capacity was reduced, as in Fig. 6. However, at very high loading rates (a crack opening displacement (COD) rate of approximately 3000 mm/s), the pullout resistance in terms of bond strength, pullout energy, and slip capacity of the flat-end steel fibers decreased due to their fracture. Since the pullout resistance of fiber deteriorates when the failure mode changes from pullout to fracture, the tensile strength and aspect ratio of steel fibers must be properly designed to prevent fracture during pullout by considering the DIF of the bond strength. Banthia and Trottier [59] also examined the pullout resistance of various steel fibers embedded in cement paste and mortar under hammer impacts. Their study [59] found higher peak pullout loads for deformed (hooked and crimped) steel fibers under impact loads than under static loads, and that the deformed fibers in cement paste were less sensitive to stress-rate than those in cement mortar, which might be related to the homogeneity of the paste. The hooked steel fibers embedded in both cement paste and mortar exhibited increased pullout energy absorption capacities under impacts, whereas the crimped fibers showed both higher and lower energy absorption capacities under impacts as compared to under static loads, due to the change in failure mode from pullout to fracture. Accordingly, they [59] commented that the fiber pullout failure mode greatly affects the energy absorption capacity of deformed steel fibers under impacts. Banthia [33] reported that the deformed steel fibers provided a higher loading rate sensitivity as compared with straight (or smooth) steel fibers, as well as smaller slips at a higher rate. The latter was inconsistent with findings from Pacios et al. [58], which noted that higher slips of straight steel fibers were obtained under impacts than static loads.

5.1.2. Flexural behaviors

Several researchers [38,60] have reported that the flexural strength of FRC with straight steel fibers greatly increased with loading rates. Suaris and Shah [38] found that the flexural strength of mortar that includes straight steel fibers was slightly more sensitive to strain rate as compared to that of plain mortar, and Naaman and Gopalaratnam [60] also reported an almost threefold increase in flexural strength of straight steel FRC (SFRC) beams as the strain-rate increased from 0.5×10^{-5}/s to 1.2/s. The inconsistent results between the pullout resistance of single fibers and flexural strength are mainly caused by factors associated with apparent bond strength [60], considering various inclination angles of the fibers. For example, when the straight steel fibers are inclined, mechanical bond components in addition to the frictional bond component are obtained, owing to the bearing of fiber on the matrix. Since the bond strength of aligned deformed steel fibers

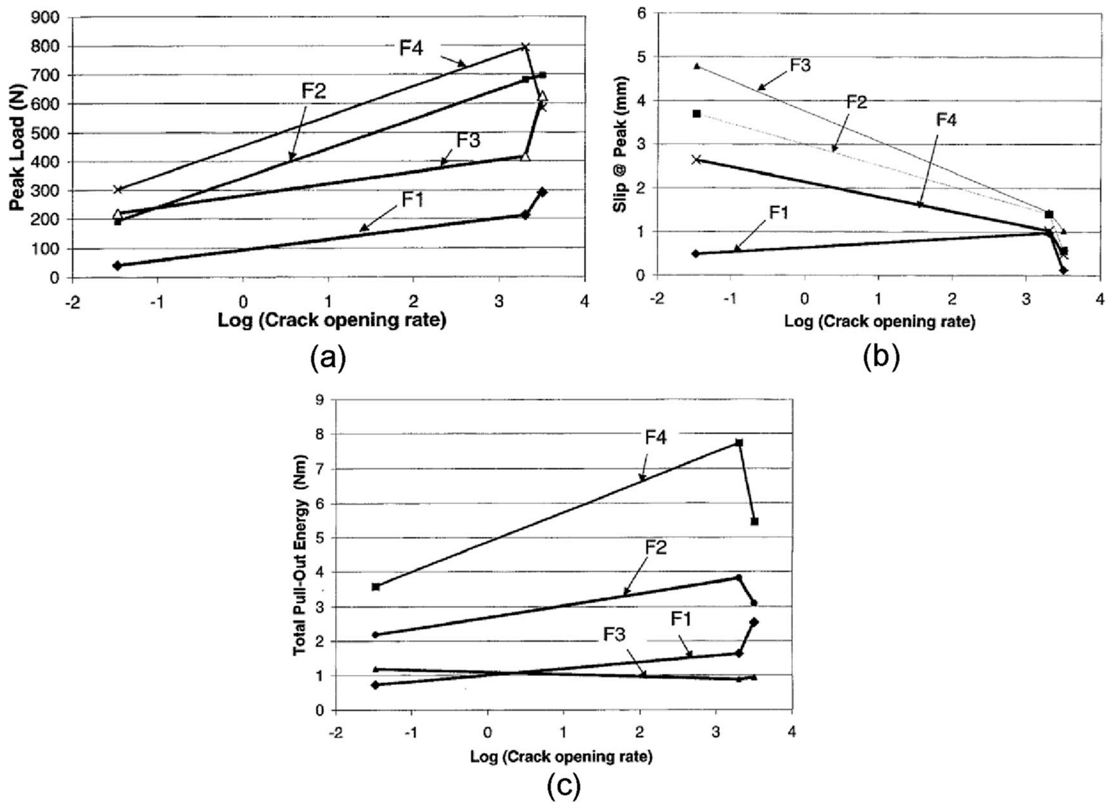

Fig. 6. Pullout behaviors [6]; (a) peak pullout load, (b) slip capacity, (c) pullout energy (F1: undeformed polyolefin fiber, F2: short crimped polypropylene fiber, F3: long crimpled polypropylene fiber, and F4: flat-end steel fiber).

increases with loading rate, consequently, the additional mechanical bond component of inclined straight steel fiber resulted in rate sensitivity. The SFRC beams obviously include fibers with various inclination angles along the tensile load direction.

Mindess et al. [54] studied the crack growth resistance of SFRC using impact testing and high-speed images and observed that steel fibers decrease crack velocity under impact loads, resulting in concrete with increased impact toughness. According to the drop-weight impact test for concrete slabs performed by Ong et al. [61], the impact resistance of plain concrete slabs greatly improved by including hooked steel fibers and increasing their amount. This is consistent with the findings from Yoo et al. [2] that the impact resistance and residual performance of concrete beams improved with the addition of hooked steel fibers and their increased volume fraction. Similar observations were also reported by Wang et al. [62] for ordinary concrete and Wang and Wang [63] for lightweight concrete. The impact resistance (including strength and energy absorption capacity) of lightweight concrete improved with the addition of steel fibers [63]. Wang et al. [62] noted that the optimum impact resistance/cost ratio was achieved with a hooked steel fiber content of 0.75% because the fracture energy absorption capacity of concrete significantly increased for fiber volume fractions of 0.5%–0.75%. Post-cracking flexural strength clearly increased when including the steel fibers, due to the fiber bridging effect [2]. Slab integrity after impact and cracking behaviors were improved for SFRC slabs compared with plain concrete slabs [61]. Hooked SFRC slabs with 0.5%, 1%, and 2% fiber volume fractions showed fracture energies approximately 2.2, 3.2, and 4.6 times higher than those of plain concrete slabs. Suaris and Shah [38] reported that the energy absorbed by SFRC with 1.2 vol% steel fibers under flexural impacts was approximately 20–100 times higher than that absorbed by plain concrete. These results indicate that the addition of deformed steel fibers increases the energy absorption capacity of concrete, but the degree of improvement in energy absorption capacity from including steel fibers is inconsistent across studies due to several parameters like machine characteristics, loading configurations (compression, tension, and flexure), fiber properties, the magnitude of imparted energy, and loading rate.

Banthia et al. [21] similarly pointed out that the energy absorption capacity of plain concrete varies greatly with different impact test machines because, especially for brittle materials, a considerable portion of the hammer impact energy is dissipated by machine vibrations, and machines with higher capacity lose more energy in this way. Banthia et al. [16,64,65] investigated the impact resistance of wet-mix shotcrete beams and plates with and without deformed (i.e., hooked, flat, and twin-coned) steel fibers. Based on the drop-weight impact test results, they reported that including deformed steel fibers improved the fracture energy absorption and toughness of wet-mix shotcrete, but the improvements are not as pronounced as those under static loads. Hooked steel fibers most significantly improved the energy absorption capacity under impact, followed by the flat and twin-coned fibers, which indicates that the impact resistance of shotcrete with steel fibers is influenced by the fiber geometry. This is consistent with the findings from Murali et al. [66] that slightly better impact resistance in terms of absorbed energy is obtained for concrete with hooked steel fibers than that with crimped steel fibers. According to impact test results performed by Wang et al. [62], very similar energy absorption capacities were observed for SFRC beams including 0.75 vol% hooked and crimped steel fibers under drop-weight impact loads. In fact, the differences between hooked and crimped steel fibers on impact resistance were relatively minor as compared with the differences between the hooked and flat or twin-cone fibers.

Nili and Afroughsabet [67] have examined the combined effect of silica fume and hooked steel fibers on impact resistance of concrete. The addition of silica fume or steel fiber increased the number of blows at first crack and failure of normal- and high-strength concretes, respectively. In addition, the inclusion of silica fume in SFRC also led to

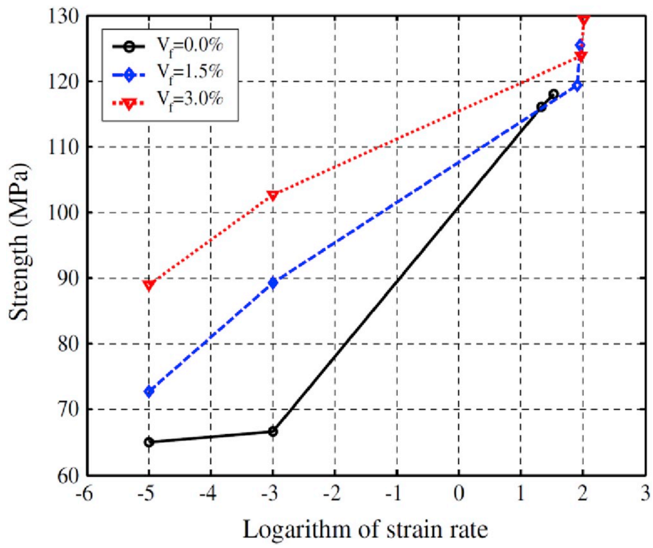

Fig. 7. Effects of steel fiber volume content and strain-rate on compressive strength of concrete [77].

an improved impact resistance, and as a result, they recommended using silica fume and steel fibers in concrete simultaneously to improve post-peak resistance and ductility under impact loads. Similar results were also reported by Ramadoss and Nagamani [68]. They [68] mentioned that the resistance of concrete under repeated impacts greatly improved by including 0.5–1.5% crimped steel fibers and positive interactions between silica fume and steel fibers was observed. The maximum impact strengths at first crack and failure of the concrete that includes crimped steel fibers were 1.51 and 1.79 times higher those of concrete without fibers.

Based on micromechanical and advanced multilayer sectional analysis, first introduced by Armelin and Banthia [69], Banthia [33] tried to predict the impact flexural response of SFRC beams. They modeled the pullout load versus slip behaviors of aligned and inclined flattened end steel fibers under impacts based on Ramberg-Osgood functions, and considered the stress-rate sensitivity on strength increases. The proposed model predicted the peak load and toughness well. However, the true post-cracking impact response of an SFRC beam was not reflected in the analytical curve, because of missing crack growth information in the model.

5.1.3. Tensile behavior

Banthia et al. [21] examined the effects of matrix strength (38–90 MPa) and deformed steel fiber geometry (hooked, crimped, and twin-cone) on the resistance of concrete under tensile impacts. At a fiber dosage rate of 40 kg/m^3, tensile strengths and fracture energies were higher for SFRC under both impact and static loads compared with plain concrete. The increase in tensile strength under impact became more pronounced with increasing compressive strength and deformed steel fiber content. However, the increase in fracture energy under impact was far more pronounced for plain concrete than for SFRC. In addition, the effectiveness of deformed steel fibers in improving the energy absorption capacity of concrete under impact and static loads diminished with increasing matrix strength because the fiber fracture and matrix splitting were more pronounced at higher matrix strengths [70]. Similarly, reductions in post-peak ductility for high-strength and ultra-high-strength SFRC were observed due to the fracture of deformed steel fibers [30]. Hao and Hao [71,72] investigated the static and dynamic splitting tensile behaviors of concrete with and without spiral steel fibers. They [71] used an SHPB test machine and high-speed camera to evaluate cracking behaviors under impact loads, exhibiting strain rates between 2/s and 20/s. The addition of spiral steel fibers obviously improved the splitting tensile strength and energy absorption under both static and impact loads. A content of 1.5% spiral steel fibers effectively inhibited crack opening under impact; for example, a COD of SFRC with 1.5% spiral steel fibers was as small as 8% of that of plain concrete at the strain of 170 μs. This ability to maintain its integrity was the main reason for improving the energy absorption capacity of SFRC.

Pająk [73] noted that the addition of steel fibers decreases the strain-rate sensitivity of cement-based composites under tensile impact. The addition of 1.5% and 2% steel fibers subtly decreased the DIF. However, at a fraction of 6 vol% steel fibers, there was a pronounced decrease in DIF at the same strain-rate. This result is inconsistent with the findings from Hao and Hao [71], who examined the rate sensitivity on the splitting tensile strength of plain concrete and SFRC using the SHPB test. In their study, the rate sensitivity of the splitting tensile strength increased with the inclusion of spiral steel fibers up to 1.5%. However, neither paper explained why the SFRC exhibited lower or higher sensitivity compared with plain concrete. Further study is required to reasonably explain this discrepancy.

5.1.4. Compressive behavior

Wang et al. [47,74,75] studied the dynamic compressive behaviors of plain concrete and steel and polyethylene (PE) FRCs using the SHPB test. In their study [47], higher compressive strengths of SFRC were obtained at higher strain-rates. In addition, the number of fractured steel fibers in the concrete increased with strain-rate, meaning that the failure mode of the steel fiber changed from pullout to fracture at increased strain-rates. The fiber fracture failure mode limited the improvement of post-peak ductility under impact loads. Wang et al. [76] similarly examined the dynamic compressive behavior of SFRCs that include 0%, 3%, and 6% very short straight steel fibers using a SHPB test machine up to a strain rate of 100/s. In their study, compressive strength also increased with strain rate, and as was expected, higher strength was obtained at higher fiber volume fractions. This result is consistent with the findings from Wang et al. [77] for SFRCs that include 0%, 1.5%, and 3% short straight steel fibers under high strain rates from 20/s to 90/s, as shown in Fig. 7, and from Yet et al. [78] for SFRCs with 0.5%, 1.0%, and 1.5% hooked steel fibers under strain rates from 30/s to 60/s. Thus, note that both the fiber volume fraction and loading rate exert significant effects on the dynamic compressive strength of SFRC. In addition, the use of steel fibers significantly improved compressive toughness under impact loads, and the effectiveness increased with the fiber volume fraction up to 3% [77]. The compressive strength and elastic modulus of fiber-reinforced high-strength concrete (HSC) with straight steel and PE fibers were less sensitive to strain-rate, yielding lower DIF values at identical strain-rates as compared with plain HSC subjected to high strain-rates from 40/s to 300/s [74]. This is consistent with findings from Pająk [73] that reported that the strain-rate sensitivity of cement-based materials decreased with increasing steel fiber volume because of the slower crack velocity obtained in fiber-reinforced HSC than in plain HSC and the lower strain-rate sensitivity of steel fibers than the concrete matrix. The main mechanism of the observed dynamic strength enhancement of concrete or concrete-like materials under SHPB tests is lateral confinement from contact surface friction and lateral inertia under high compressive loading rates [15,79]. The SFRC was almost insensitive to strain-rate when the volume fraction of steel fibers was greater than 6% [79]. Interestingly, increased critical strain, which is the strain corresponding to maximum stress, was observed in the HSC that included straight steel fibers compared to the plain HSC. According to Bischoff and Perry [80], the extent of cracks for failure increased with the strain-rate. In addition, lateral internal confinement generated by high volume fractions of steel fibers, led to the formation of significant microcracks, but limited the formation of macrocracks, as reported by a previous study [10]. The CEB-FIP [81] model underestimated the DIF of the compressive strength of plain HSC, whereas it overestimated the DIF of the compressive strength of HSC that included fibers [74].

Lok and Zhao [12] examined the dynamic compressive behaviors of hooked SFRC using the SHPB test. The compressive strength of SFRC increased with strain-rate, which is similar to that of ordinary concrete and consistent with the findings from Xu et al. [82]. The effect of the deformed shape of steel fibers on dynamic compressive properties of concrete was investigated by Al-Masoodi et al. [83]. In their study [83], γ- and W-shaped steel fibers provided greater compressive strengths under 2 and 3 MPa impact pressures as compared with plain concrete and conventional hooked SFRC. In particular, the specimen that included W-shaped fibers provided the highest ultimate strain and toughness at both 2 and 3 MPa pressures. Marar et al. [84] also evaluated the dynamic compressive toughness of hooked steel fiber-reinforced HSC with various aspect ratios (60, 75, and 83) and volume fractions (0.5%, 1.0%, 1.5%, and 2.0%) using a drop-weight impact testing machine, and reported that the compressive toughness and impact energy of high-strength SFRC improved by increasing the fiber content and aspect ratio.

Fujikake et al. [85] studied the dynamic properties of cement mortar with steel fibers under high loading rates and triaxial stress states. The volume fractions of steel fibers ranged from 0% to 4%, and the confining pressures and strain-rates ranged from 0 MPa to 70 MPa and from 1.2×10^{-5}/s to 2/s, respectively. By including the steel fibers, the failure mode of high-strength cement mortar changed from a mixed mode accompanied by splitting failure to shear slip failure under both static and impact loads, since the fibers provided a confinement effect. Given the confining pressure by steel fibers, the dynamic failure criterion under high strain-rates and triaxial stresses predicted the maximum strength of cement mortar that includes steel fibers.

5.1.5. Projectile impact resistance

With the addition of hooked steel fibers in concrete slab mixtures, the resistance to damage around a penetration crater by a projectile impact improved, and the residual velocity of the projectile after penetration was markedly reduced [86]. The reduced crater volume of SFRC plates at both the front and rear was experimentally observed by Almansa and Cánovas [87], compared to that of plain concrete plates. Reduced front and rear craters and total weight loss were also observed by Dancygier et al. [88] for HSC panels with hooked steel fibers. In addition, perforation resistance increased up to 60% by including 60 kg/cm^3 steel fibers, whereas the increase in fiber content from 60 to 80 kg/cm^3 in the rear of slab did not improve perforation resistance. Enhanced perforation resistance by including steel fibers, as reported by Dancygier et al. [88], is inconsistent with the finding from Zhang et al. [89] noting that the addition of 1.5 vol% steel fibers substantially reduced crater diameter (to approximately 40–80% lower than that of plain concrete) and crack propagation, but did not have a significant effect on penetration depth. Based on Almansa's examination [87] of the projectile impact resistance of normal concrete and SFRC including 0.5, 1.0, and 1.5 vol% hooked steel fibers, the addition of hooked steel fibers only slightly decreased the thickness of the plain concrete plate required to avoid perforation, but significantly reduced the thickness needed to avoid scabbing and endure multiple hits by projectile impacts. Furthermore, Luo et al. [90,91] reported the higher impact resistance of SFRC under projectile impact compared with that of steel-bar-reinforced HSC. Smash failure of the reinforced HSC specimen was prevented by including steel fibers, and the SFRC specimens exhibited several radial cracks in the front faces by projectile penetration and some minor cracks in the side surfaces. Consequently, although there are conflicting results, it can be generally noted that incorporating steel fibers is more effective in reducing the area of craters or scabbing than penetration depth.

5.2. Polymeric fibers

5.2.1. Fiber pullout behavior

The pullout energy and bond strength of deformed PP fibers continuously increased with the loading rate, whereas the slip capacity was reduced [6], as shown in Fig. 6. This stiffening (lower slip capacity) is beneficial for decreasing the maximum crack width at the peak load for PP FRC. A drastic increase in the pullout energy of straight PP fibers was also obtained by Naaman [57] from loading velocities approximately from 1×10^0 cm/s to 300 cm/s. This is inconsistent with the pullout energy of straight steel fibers, which is independent to loading velocity. In addition, since the strength of the PP fiber itself was rate sensitive, a mixed failure mode (fracture or pullout) was strongly dependent on the loading rate.

5.2.2. Flexural behavior

Banthia et al. [64] reported that superior static and impact resistances were obtained when longer straight PP fibers were incorporated compared to short ones. In addition, the shotcrete including crimped PP fibers exhibited better energy absorption capacity under both static and impact loads compared to that with straight PP fibers, because of their higher pullout resistance. Based on Toutanji's study [92], the impact resistance of PP FRC substantially improved with increasing the amount of silica fume incoporated, which helped to better disperse fibers. The optimal silica fume content was determined to be 10% for FRC with PP fibers with a length of 19 mm. Nili and Afroughsabet [93] also evaluated the effects of silica fume and PP fibers on the impact resistance of concrete, according to a free falling ball test. The number of blows at first crack and concrete failure, indicating impact resistance, significantly increased by including 0.2%, 0.3%, and 0.5% PP fibers by 31%, 100%, and 360%, respectively, at first crack and by 42%, 107%, and 376%, respectively, at failure. This result is consistent with findings from Manolis et al. [94], Song et al. [95], and Soroushian et al. [96]. Manolis et al. [94] evaluated the effect of PP fibers on the impact resistance of concrete using the free falling ball test and reported that the number of blows required to cause initial cracking and failure all increased by including PP fibers up to 5%. Similarly, Song et al. [95] experimentally verified that the first crack and failure strengths of 0.6 kg/m^3 PP FRC were 11.9% and 17.0% higher than those of plain concrete. However, in their study [95], nylon fibers were more effective in improving the impact resistance of concrete than an identical amount of PP fibers (0.6 kg/m^3). For instance, the addition of 0.6 kg/m^3 nylon fibers into a concrete mixture led to 19.0% and 30.5% higher first crack and failure strengths under impact loads as compared with plain concrete. Mindess and Vondran [97] also reported that the addition of PP fibers enhanced impact resistance for both flexural strength and fracture energy. 0.5 vol% PP FRC had a flexural strength and fracture energy approximately 40% and 100% higher, respectively, than plain concrete under a drop-weight impact with a velocity of 2.95 m/s. In addition, Mindess et al. [98] noted that normal concrete with 0.5 vol% fibrillated PP fibers with a length of 37 mm exhibited higher fracture energy and fracture toughness than plain normal concrete and HSC without fibers. The HSC produced lower fracture energy and toughness than the normal-strength concrete due to its greater brittleness, and regardless of the strength and existence of fibers, the fracture energy and toughness significantly increased with the loading rate. In contrast, as compared with other researchers [93,94], Alhozaimy et al. [99] published test results indicating that the number of blows at first crack was not obviously influenced by the addition of PP fibers, but that the number of blows at failure improved up to a PP fiber volume fraction of 0.2%.

The effectiveness of adding PP fibers in increasing impact resistance decreased with the water-to-cement ratio, indicating higher strength concrete. The increased brittleness of concrete from including silica fume was mitigated by adding PP fibers, and the ability of silica fume concrete to absorb kinetic energy from a hammer drop improved considerably with the addition of PP fibers [92]. A considerable increase in the fracture energy of reinforced concrete beams by adding PP fibers under impact was also reported by Mindess et al. [100], and the fracture energy was much greater for the concrete beams reinforced with PP fibers and steel rebar simultaneously as compared with the sum of the effects of PP fibers and steel rebar considered separately. This means that there was a synergetic effect of using both the steel rebar and PP fibers. On the other hand, the addition of PP fibers did not have a noticeable effect on the first natural frequency of concrete slabs because of the insignificant changes in the specimen mass and static stiffness [94], and the flexural strength of concrete under drop-weight impact was not affected by the fibrillated PP fibers [100].

Dey et al. [31] also evaluated the impact response of aerated concrete with and without PP fibers under a drop-weight impact load. In their study [31], dynamic flexural strength was found to be more than 1.5 times higher than static strength, due to the strain-rate effect. The strain-rates applied by the hammer drop ranged from about 0.02/s to 22.4/s. Interestingly, similar flexural strength was obtained for aerated concretes with and without PP fibers, but the one with 0.5 vol% PP fibers showed flexural toughness 3 times higher than the one without fibers. The drop-weight impact test method is good for quantitatively evaluating the impact resistance of cement-based materials like aerated concrete for masonry products.

The impact resistance of plain concrete improved by using polyvinyl alcohol (PVA) fibers [16,64,101,102]. The addition of high volume fractions of PVA fibers changed the impact failure mode from a brittle pattern to ductile one, causing a great increase in impact toughness [102]. However, this improvement was insignificant as compared with those adding steel and PP fibers [16,64]. This is because a relatively brittle failure mode was obtained for the FRC with deformed PVA fibers, as compared with those including steel and PP fibers, due to an increase in fiber fracture under impact.

Foti and Paparella [103] have performed impact tests for concrete slabs with and without polyethylene terephthalate (PET) fibers. The discrete, long PET fibers were included in the concrete slab as reinforcement, and a metallic cylinder was dropped at the center of the slab. The slab reinforced with PET fibers did not completely fail from the impact, whereas the slab without fibers completely failed, confirming the improvement of impact resistance in FRCs. In addition, a good adhesion between the PET fibers and concrete was observed, even after the presence of cracks.

5.2.3. Compressive behavior

Al-Masoodi et al. [83] have reported that by including PP fibers, dynamic compressive strength and toughness were improved as compared with plain concrete. Similar to the results reported by Banthia et al. [64], the addition of PP fibers has less influence on the static properties of plain concrete, whereas it greatly improved the dynamic compressive properties. Thus, the use of PP fibers under impact is more effective in improving the mechanical properties of concrete than under static loading conditions. The dynamic compressive behaviors of HSC that includes PE fibers were also evaluated by Wang et al. [74] using the SHPB test method. The applied strain-rates ranged from 40/s to 300/s, and 0.5 vol% PE fibers were included in an HSC mixture having a static compressive strength of about 80–90 MPa. In static loading conditions, there was no significant effect of including 0.5% PE fibers in the HSC mixture, as in the results reported by previous studies [64,83]. However, a lower compressive strength and elastic modulus were found for the PE fiber-reinforced HSC compared to the plain HSC under impact, which is inconsistent with the previous findings [64,83]. Lower DIF values of the compressive strength and elastic modulus were also observed in the PE fiber-reinforced HSC than in its counterpart without fibers, owing to the slower crack velocity [74]. This discrepancy might be caused by different concrete strengths and fiber types, but to draw a clear conclusion on the effect of polymeric fibers on the dynamic compressive behaviors of concrete, further study that considers various concrete strengths and polymeric fibers is needed.

5.3. Carbon fibers

Banthia and Ohama [104] noted that the impact resistance (i.e., tensile strength and fracture energy) of plain concrete improved after adding carbon fibers; this enhancement was proportional to the volume fraction of carbon fibers up to 5%. The addition of silica fume was also effective in dispersing carbon fibers in the matrix. Similar results were also reported by Ohama et al. [105] and Tabatabaei et al. [106]. Ohama et al. [105] examined the impact resistance of cement composites reinforced with carbon fibers and silica fume using JIS A 1421 (a free-falling steel ball test). In their study [105], an 80-g steel ball was dropped on plate specimens made of carbon-fiber reinforced composites (100 mm × 100 mm × 10 mm) from a height of 20 cm and measured the number of blows up to complete failure. The plain specimen failed after only one blow, whereas the composite with 5 vol% carbon fibers did not break even at more than 3000 blows, indicating that impact resistance was substantially improved by including carbon fibers. In addition, regardless of carbon fiber length, impact resistance increased with the volume fraction up to 5%. In the same manner, Tabatabaei et al. [106] reported that the blast resistance of RC panels was greatly enhanced by including 1–1.5% 100-mm-long carbon fibers. They further found that the addition of carbon fibers effectively reduced the vibrations of concrete under dynamic loads of low magnitude and high frequency as they increased the concrete's damping ratio [107].

However, at very high loading rates (a strain-rate of 0.71/s by drop hammer freefall), energy absorption capacity in shotcrete including micro carbon fibers decreased compared with that of plain shotcrete [64], mainly because of carbon fiber's fractures. Since the coarse aggregate included in concrete mixtures normally adversely affects FRC that includes micro fibers, it was eliminated in a previous study [64]. Nevertheless, there was no improvement in the impact resistance due to the fiber fracture. Therefore, it is concluded that in order to improve the impact resistance of concrete by including carbon fibers, the mixture of carbon FRC must be properly designed to prevent the fracture of carbon fibers. In other words, the normal-strength concrete mixture may be more proper for making impact resistant carbon FRCs than the HSC mixture.

5.4. Basalt fibers

Li and Xu [13] investigated the impact resistance of geopolymeric concretes (GCs) with static compressive strengths of 26.2, 44.1, and 56.4 MPa, with and without basalt fibers. In this study, they employed a 100-mm-diameter SHPB test machine and applied strain-rates from 10/s to 100/s. The addition of basalt fibers (v_f of 0.1–0.3%) significantly improved the deformation and energy absorption of plain GCs, but there was no obvious enhancement in dynamic compressive strength. Li and Xu [108] also examined the effects of basalt fibers and strain-rate (30–100/s) on the dynamic compressive behavior of GC using the same SHPB machine and reported that the impact properties of basalt fiber-reinforced GC—including dynamic compressive strength, critical strain, and specific energy absorption—increased almost linearly with the average strain rate. In addition, the optimum volume fraction of basalt fiber was suggested to be 0.3% by Li and Xu [108], which increased the special energy absorption of GC from 8.9% (at 40/s) to 13.2% (at 100/s). Other researchers [109] also reported that the inclusion of 0.1 vol% basalt fibers increased the dynamic compressive strength and energy absorption capacity of ordinary concrete by up to 26% and 14%, respectively, and the strengthening effect of basalt fibers was more significant than that of carbon fibers for ordinary concrete.

5.5. Natural fibers

Ramaswamy et al. [110] examined the effect of natural fibers such as jute, coir, and bamboo, on the impact resistance of concrete under free falling impact loads. The impact energy at first crack and number of blows for failure all increased with a natural fiber volume fraction of 1%. For instance, the impact energy for the first cracking of FRC with natural fibers was higher than that of plain concrete by approximately 10–20%. In addition, jute and coir fibers gave slightly better impact resistance than bamboo fibers for both slab and beam specimens.

de Andrade Silva et al. [111] also investigated the impact resistance of unidirectional continuous sisal fiber-reinforce cement composites using a free-falling impact test machine. Their experimental results indicated that sisal fiber-reinforced cement composites led to insignificant changes of flexural strength according to the strain-rate ranging from static to impact (3.8/s – 5.8/s) conditions. However, with the change in load, the dissipated specimen energy increased, and the ratio of total absorbed energy to impact energy was found to be between 0.25 and 0.44. As compared with alkali resistant (AR) glass fabric-reinforced composites [112], the composites with sisal fibers provided a more ductile behavior under impact and a similar ultimate impact strength. Furthermore, based on Zhu's study [112], the total absorbed energy of AR glass fabric-reinforced composites increased with hammer drop heights, while the ratio of absorbed to potential energy decreased.

5.6. Hybrid fibers

Song et al. [113] statistically examined the impact resistance of steel-PP hybrid FRC based on the ACI Committee 544 free falling ball test, and reported that the impact strength of steel-PP hybrid FRC was slightly higher than that of single SFRC, which is consistent with findings from Wang et al. [114]. Based on a Kaplan-Meier analysis, they [113] also concluded that the hybrid FRC had slightly more reliable first-crack and failure strengths than the SFRC. In the same vein, the superior impact resistance of steel-PP or steel-glass FRC over hooked SFRC was also reported by Yildirim et al. [115]. Based on drop-weight impact test results from Mo et al. [116], the impact resistance of hybrid FRC was better than that of SFRC at a constant fiber fraction of 1 vol%. However, the better impact resistance was only achieved when a small amount of steel fibers were replaced with PP fibers. Hybrid FRC with 0.9% steel + 0.1% PP fibers provided the best impact resistance, including impact energy of 17 kJ, which is 1.6 and 60 times higher than those of SFRC and plain oil palm shell concrete, and an impact ductility index of 42, which is 1.9 and 8.4 times higher than SFRC and plain concrete. In addition, Banthia and Nandakumar [117] reported that the effectiveness of using deformed steel fibers to improve the crack growth resistance and fracture energy of concrete is enhanced by including secondary PP fibers. The enhanced impact resistance of hybrid FRC can result in its effective use in blast shelters and earthquake resistant structures.

Almusallam et al. [24,118] also evaluated the effectiveness of using hybrid steel and plastic fibers on the projectile impact resistance of reinforced normal- and high-strength concrete slabs using an air-gun system. They adopted fiber volume fractions from 0.6% to 1.4%, and some portion of the hooked steel fibers was replaced with PP and Kevlar fibers to make hybrid FRC. In their earlier study [24], the hybrid fibers' inhibition of crack development led to a reduction in the area of spalling and scabbing damage to concrete slabs under projectile impact, whereas the penetration depth was not greatly affected by fiber type or amount. The slab with steel fibers exhibited better impact resistance than that with PP fibers, indicating that the use of steel fiber is more effective in improving projectile impact resistance. In the same vein, for hybrid fibers, better impact resistance was achieved when only a small amount of the steel fibers were replaced with PP fibers. The optimum volume proportion of steel and PP fibers was suggested as 2:1.

The hybrid effect of steel and PE fibers on the dynamic compressive behaviors of HSC was also examined by Wang et al. [74]. The effect of adding 0.5% steel and 0.5% PE fibers on static compressive strength was insignificant, but a lower compressive strength and elastic modulus were obtained under impacts (strain rates of 40–300/s) as compared with plain HSC. HSCs including either steel or PE fibers exhibited similar strain-rate sensitivity on compressive strength to HSC with hybrid steel-PE fibers, but a much smaller critical strain, along with a slightly higher elastic modulus. Most importantly, the highest dynamic toughness was found when using hybrid steel-PE fibers, followed by steel and PE fibers.

Dawood and Ramli [119] investigated the effect of hybrid steel, palm, and synthetic fiber reinforcements on the impact resistance of high-strength flowable concrete using the free falling ball test. They applied an identical 2 vol% of fiber for all test specimens, and some portion of the steel fibers were replaced with palm and synthetic fibers. The top two impact resistances were obtained for hybrid FRCs with 1.75 vol% steel fiber + 0.25 vol% palm fiber and 1.5 vol% steel fiber + 0.25 vol% palm fiber + 0.25 vol% synthetic fiber, respectively. These hybrids provided better impact resistance at both first crack and failure as compared with 2 vol% single SFRC. However, as more steel fibers were replaced with palm and synthetic fibers, a significant deterioration in impact resistance was obtained, and thus, they concluded that only a small amount of steel fibers can be replaced with palm and synthetic fibers to retain the benefit to impact resistance. The hybrid FRC (1.75 vol% steel fiber + 0.25 vol% palm fiber) showing the best impact resistance required 25 times more blows for first crack appearance than plain concrete, and the percentage increase in the post-cracking zone was 78.6%, implying that hybrid fiber reinforcement is effective in improving impact resistance at both before and after cracking.

Lastly, Banthia et al. [44] investigated impact resistance of mortar and concrete beams reinforced with single and hybrid steel and carbon fibers under normal and subnormal temperatures (22 °C and −50 °C). This study adopted macro- and micro steel fibers, and micro carbon fiber. Test results indicated that the hybrid use of 1 vol% macro steel fiber and 1 vol% micro steel fiber was more effective in improving impact energy absorption capacity compared with either alone. Furthermore, the addition of 1 vol% micro steel and micro carbon fibers improved the fracture energies of SFRC beams under impact loads, due to their synergetic effect, and a marginal decrease in impact resistance was observed at −50 °C.

6. Comparative impact resistance of FRCs with various fibers

6.1. Steel fibers vs. polymeric fibers

Bindiganavile and Banthia [6] examined the pullout resistance of a straight polyolefin (PO) fiber, a sinusoidally deformed PP fiber, and a flat-end steel fiber in concrete with a 28-day compressive strength of 40 MPa. A higher pullout resistance was measured when using the steel fibers up to a COD rate of 2000 mm/s. The bond strengths of all polymeric fibers increase with loading rate, but the steel fiber showed a decrease in bond strengths at very high loading rates (COD rates of 2000–3000 mm/s), because it was fractured. At very high loading rates, the highest pullout resistance was observed in the deformed PP fiber, followed by the steel and PO fibers, as shown in Fig. 6a. Furthermore, slip capacity decreased with increasing loading rate for both polymeric and steel fibers (Fig. 6b). However, the PP fibers produced the most significant decrease in the slip capacity with loading rate, and this stiffening could effectively reduce the maximum crack width at the peak load. They [6] thus concluded that, at very high loading rates, the pullout resistance and slip capacity of PP fibers can approach those observed in steel fibers. In the same vein, Gokoz and Naaman [55] reported the higher loading rate sensitivity on the tensile strength of PP fibers as compared to those of steel and glass fibers, as shown in Fig. 8. All of the steel fibers were pulled out at all velocities, while the percentages of fiber pulling out of PP fibers obviously increased with increasing the loading rate. So, the pullout percentages of PP fibers were getting closer to the value of 100% with an increase in the loading rate, owing to its higher rate sensitivity on the tensile strength. Thus, it can be noted that the use of PP fiber in ordinary concrete is more effective in enhancing the fiber bridging capacity at higher loading rates, such as impact and blast, than lower rates (quasi-static condition). For this reason, the PP fibers provided higher energy absorption capability at high loading rates than the steel fibers, as reported by Gokoz and

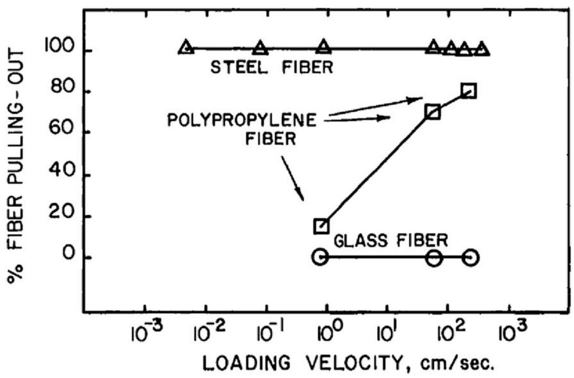

Fig. 8. Pullout percentages of different types of fibers according to the loading rate [57].

Naaman [55].

Ong et al. [61] reported that, at the same volume fractions of 0.5%, 1%, and 2%, hooked SFRC slabs provided approximately 40%, 100%, and 136% higher fracture energies than PO FRC slabs respectively, and approximately 19%, 53%, and 80% higher fracture energies, respectively, than PVA FRC slabs. PVA fibers were more effective in improving the fracture energy capacity of concrete compared to that of PO fibers at the identical volume fraction. As shown in Fig. 9, the addition of hooked steel fibers gave significantly superior performance with regard to multiple cracking behavior, resistance to shear cone formation, and slab integrity after impact, as compared with polymeric (i.e., PO and PVA) fibers. Similarly, based on the impact test results performed as per ACI Committee 544 [120], Nia et al. [19] have reported that hooked steel fibers exhibited a better impact resistance in both normal- and high-strength concretes as compared to PP fibers. They evaluated impact resistance by counting the number of blows to final fracture. Concrete with steel fibers exhibited higher impact resistance than that with PP fibers due to the steel fiber's larger length, greater tensile strength, and better cohesion [19]. Wang et al. [62] similarly reported that hooked steel fibers more greatly increased the fracture energy of concrete beams under impact than PP fibers at low volume fractions (up to 0.5%); Banthia et al. [16,64,65] also demonstrated that the inclusion of steel fibers provided the greatest improvement in toughness for wet-mix shotcrete beams and plates under both static and impact loads, as compared with PP and PVA fibers. In addition, as compared with PVA fibers, PP fibers produced better impact resistance in terms of energy absorption capacity [16,64]. Bindiganavile and Banthia [35] also noted that macro steel fibers exhibited superior crack growth resistance (greater stress intensity) under both static and impact loads compared with micro PP fibers, as shown in Fig. 10. A much larger stress intensity factor, K_I, was obtained in SFRC over PP FRC and ordinary concrete. In addition, much higher K_I values were obtained under impact loads (Fig. 10b) than under static load (Fig. 10a), which is one of the main reasons for the increase in toughness under impact loads. In a drop-weight impact test performed by Suaris and Shah [121], steel fibers were more effective in improving flexural strength than PP fibers at both static and impact loads because of the smaller bond strength between PP fibers and cement mortar. The energy absorption capacity of specimens including PP fibers was found to be only one-third that of the specimens that included long steel fibers.

Interestingly, Bindiganavile et al. [32,34,35] reported that although deformed steel fibers resulted in much higher energy absorption capacity under both static and impact flexural loads than polymeric (i.e., PO and PP) fibers, the difference between the deformed steel fibers and polymeric fibers diminished under greater impact intensities compared to those under static load, as shown in Fig. 11. Long PP fibers absorbed approximately 80% of the energy absorbed by steel fibers under impact. Therefore, they [32] concluded that PP fibers with suitable length, geometry, and deformations can absorb fracture energy very close to that observed of deformed steel fibers. In addition, at very high impact loads (incident energy = 600 J), FRC that includes crimped PP fibers exhibited higher flexural toughness than flat-end steel FRC [34] because the flexural toughness of the SFRC decreased at incident energies higher than 120 J owing to fiber fracture, whereas the PP FRC provided a continuous increase in flexural toughness with the incident energy applied up to 600 J, which was attributed to the improvement of the fiber's elastic modulus.

As reported in Wang's study [74], there was no significant effect of fiber type (steel v. PE fibers) and volume fraction on the DIF of the compressive strength of HSC. However, the compressive toughness of specimens including straight steel fibers was higher than that of those containing PE fibers [74]. By considering fabrication cost and workability, Wang et al. [74] suggested using 0.5% steel fibers to improve the impact resistance of concrete, rather than an identical amount of PE or hybrid (steel + PE) fibers.

6.2. Polymeric fibers vs. glass fibers

Yildirim et al. [115] examined the resistance of PP and glass FRCs under repeated impact loads. At the identical volume fraction of 0.1%, glass fiber was more effective in improving the impact resistance in terms of number of blows at both first cracking and failure points than PP fibers. The glass fibers exhibited better impact resistance mainly because of their higher elastic modulus, tensile strength, and aspect ratio compared with PP fibers. In addition, specimens including glass fibers were more sensitive to the strain-rate on the flexural strength as compared with specimens including PP fibers, which means that higher flexural strength under impact was obtained using glass fibers than using PP fibers. On the other hand, poorer impact resistance of the glass fiber than the PP fiber was reported by other researchers [55,121]. Suaris and Shah [121] reported that, due to the fracture of glass fibers, it exhibits the energy absorption capacity much smaller than that of PP fibers under impact load. Gokoz and Naaman [55] also noted that the

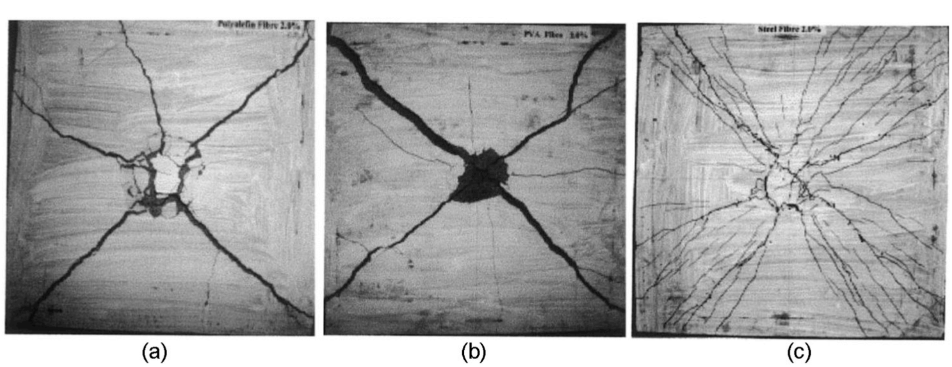

Fig. 9. Failure patterns of concrete slabs including 2% by volume of; (a) polyolefin fibers, (b) PVA fibers, (c) hooked steel fibers (bottom surface) [61].

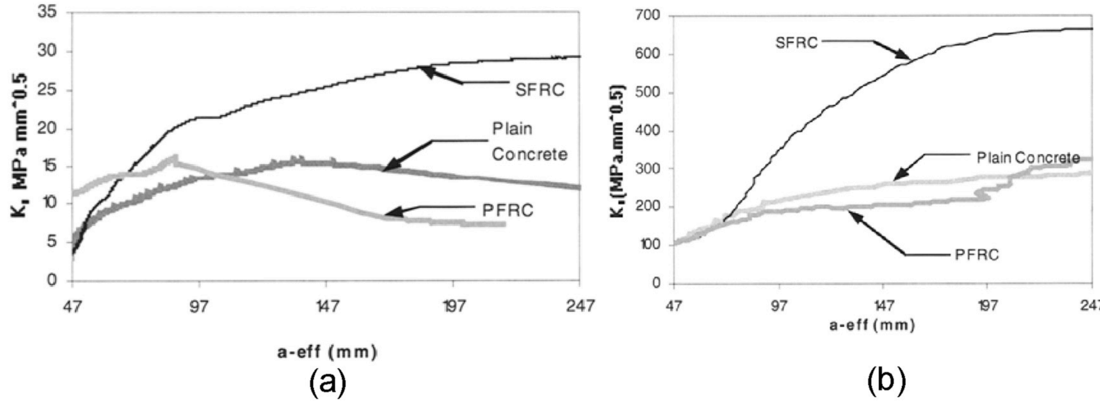

Fig. 10. Crack growth resistance of plain concrete and FRC under (a) static load and (b) drop weight impact load (750 mm drop) (Note: SFRC = FRC with steel fibers and PFRC = FRC with PP fibers) [35].

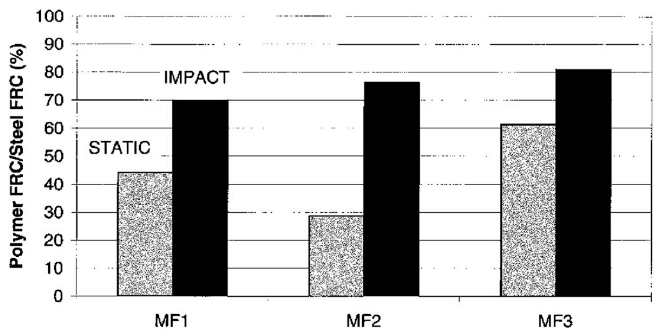

Fig. 11. Fracture energy dissipated by polymeric fibers as compared to that by steel fibers [32] (MF1 = polyolefin fiber, MF2 = polypropylene fiber (30 mm long), and MF3 = polypropylene fiber (50 mm long)).

poorer energy absorption capacity of glass fibers is obtained than that of PP fibers because of its lower rate sensitivity on the tensile strength. The percentages of pulling out of PP fibers increased at higher velocities, whereas that of glass fiber was insignificantly affected by the loading rate. So, the pullout resistance of PP fibers was much highly enhanced according to the loading rate, relative to that of glass fibers.

6.3. Steel fibers vs. carbon fibers

According to Banthia et al. [64], the impact resistance of wet-mix shotcrete that includes deformed steel fibers was much higher than that with micro carbon fibers. For instance, the fracture energies of shotcrete reinforced with hooked steel fibers were found to be 124.94–135.95 J, which is at least 18 times higher than that reinforced with straight micro carbon fibers. Similar observations were also reported by Banthia et al. [44] under both normal and low temperatures. The fracture energy absorption capacity of mortar under drop-weight impacts was higher for macro steel fibers than for micro carbon fibers. In addition, the improvement in the impact resistance of macro steel FRC was more effective when using micro steel FRC instead of micro carbon FRC. However, under low-magnitude high-frequency dynamic loads, carbon fibers were more effective in reducing the vibrations of pre-cracked concrete as compared with steel fibers, since they resulted in a higher damping ratio [107]. Hence, it is noted that steel fibers are more effective in bridging cracks and limiting crack propagation and widening under impact loads, as compared with carbon fibers, whereas carbon fibers more efficiently limit vibrations of pre-cracked concrete under small dynamic loads than steel fibers.

7. New findings on the strain-rate sensitivity of FRCs

Fig. 12a shows the relationship between the DIF on compressive, tensile, and flexural strengths and strain-rate of FRCs with various fiber types and volume fractions. It was obvious that the least loading rate sensitivity was obtained for the compressive strength, while the highest sensitivity was found from the tensile strength. The flexural strength term provided an intermediate rate sensitivity because it is subjected to both the compressive and tensile stresses in the cross section. This observation is consistent with the findings of Suaris and Shah [38] and Banthia et al. [20] for plain concrete without fibers and means that the addition of fibers into concrete does not influence the effect of loading condition on the loading rate sensitivity.

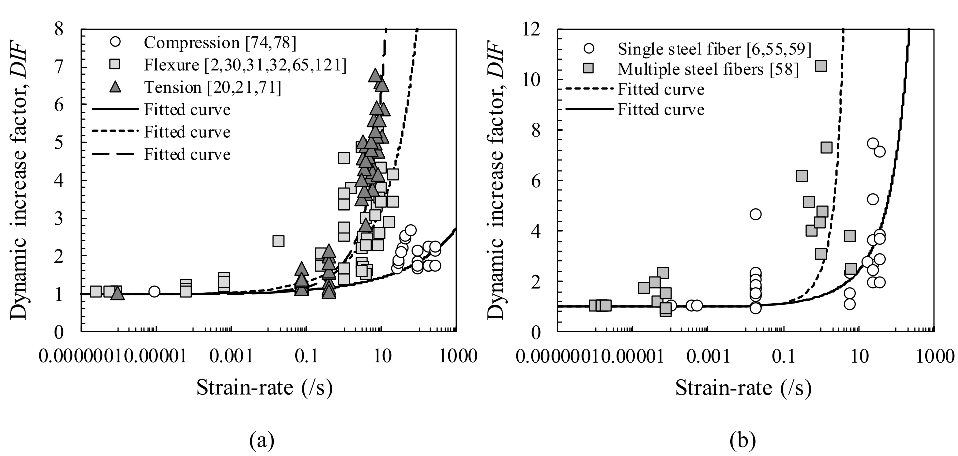

Fig. 12. Relationships between the DIF and strain-rate of FRCs according to (a) loading configuration and (b) number of steel fibers.

Naaman and Shah [122] reported interesting findings that the fiber volume fraction affects the pullout resistance of steel fibers in ordinary cement mortar. Pacios et al. [58] thus conducted static and dynamic pullout tests of using multiple straight steel fibers in cement matrix with two different fiber numbers (16 vs. 8) and reported two important findings: 1) maximum pullout load and slip capacity of multiple steel fibers increased with increasing the loading rate and 2) increasing the number of fibers, which reduces the fiber spacing, was effective in increasing the loading rate sensitivity but ineffective in the average bond strength. In order to verify this explanation, the relationships between the DIF on the bond strength and strain-rate of multiple and single steel fibers embedded in ordinary cement matrix were compared, as shown in Fig. 12b. It was obvious that a higher loading rate sensitivity on the pullout resistance of steel fibers in cement matrix is obtained when multiple fibers are adopted as compared to the single steel fiber cases. However, no scientific and reasonable explanations on the above observations have been reported yet, thus future studies require to be done.

The strain-rate sensitivity can be evaluated based on a prediction model for the DIF and strain-rate relationship. The most widely adopted model for the strain-rate effect on the compressive strength of concrete is proposed by CEB-FIP Model Code [81], and the proposed formula is given as follows.

$$DIF = \left(\frac{\dot{\varepsilon}}{\dot{\varepsilon_s}}\right)^{1.026\alpha} \quad \dot{\varepsilon} \le 30s^{-1} \quad DIF = \gamma_s\left(\frac{\dot{\varepsilon}}{\dot{\varepsilon_s}}\right)^{1/3} \quad \dot{\varepsilon} > 30s^{-1} \tag{1}$$

where $\dot{\varepsilon}$ = strain-rate (up to 300/s), $\dot{\varepsilon_s}$ = static strain-rate (30×10^{-6}/s), $\alpha = \frac{1}{5 + 9 \cdot f_s / 10}$, f_s is the static compressive strength, and $\log\gamma_s = 6.156\alpha - 2$.

Wang et al. [74] reported that the CEB-FIP model [Eq. (1)] is applicable but underestimates the DIF on the compressive strength of plain concrete and overestimates that of FRCs with various types of steel and PE fibers. The effect of adding fibers into concrete on the strain-rate sensitivity under compression is still controversial: Wang et al. [74] noted that the strain-rate sensitivity of plain HSC is higher than those of similar-strength FRCs, whereas Hao and Hao [123] found that the specimens become more sensitive to the strain-rate when the fibers are added and their volume fraction increases. Since the strain-rate sensitivity of plain concrete and FRCs is different [74,123], Wang et al. [74] insisted that a modified equation for the DIF and strain-rate relation of FRCs needs to be suggested to consider the strain-rate effect precisely when we design FRC structures or numerically simulate them. Several previous studies [12,47,123–125] have thus proposed empirical equations for the DIF on the compressive strength of FRCs and they are summarized in Table 2. Since the previous models were suggested based on the test data (empirical), most of them can be only adopted for a certain circumstance with limited ranges of matrix strength, fiber type and volume fraction. The rate sensitivity of FRC is influenced by some factors: for example, the strain-rate sensitivity of SFRC varied according to the fiber shape and volume fraction but is insignificantly affected by the matrix strength [124]. The deformed steel fibers generally provided higher rate sensitivity than that of straight one for HSC, and the rate sensitivity increased with increasing the fiber dosage from 1.5% to 2.5% but rather reduced after that up to 3.0% [124]. Thus, to properly design FRC structures subjected to the extreme loads, an appropriate prediction model, given in Table 2, is recommended to use for similar type of FRC.

The most famous empirical DIF models for concrete under tension have been suggested by CEB-FIP Model Code [81] and Malvar and Ross [126]. Among them, the CEB-FIP model [81] for DIF of tensile strength is given by the following equation.

$$DIF = \left(\frac{\dot{\varepsilon}}{\dot{\varepsilon_s}}\right)^{1.016\alpha} \quad \dot{\varepsilon} \le 30s^{-1} \quad DIF = \beta\left(\frac{\dot{\varepsilon}}{\dot{\varepsilon_s}}\right)^{1/3} \quad \dot{\varepsilon} > 30s^{-1} \tag{2}$$

where $\alpha = \frac{1}{10 + 6 \cdot f_s / 10}$ and $\log\beta = 7.11\alpha - 2.33$.

Othman and Marzouk [127] compared the DIFs on the compressive and flexural-tensile strengths of FRCs and CEB-FIP models and concluded that the CEB-FIP model [81] overestimates the compressive and tensile strength of high-strength FRC and its overestimation becomes more significant in tension. Furthermore, several researchers [71,128–130] have experimentally verified the influence of adding fibers on the rate sensitivity of tensile strength of concrete. Hao and Hao [71] and Shah [129] reported that the least sensitivity to the strain-rate is found in plain concrete under tension and the higher rate sensitivity is achieved with the higher fiber volume fraction. On the contrary, Wang et al. [130] reported that the most remarkable strain-rate effect on the tensile strength is obtained in the plain concrete without fibers and the FRC with volume fraction of 1.5% is almost insensitive to the strain-rate. Xu et al. [128] also noted that the inclusion of fibers affects the DIF of tensile strength although the fiber contents and types have a minimum influence on it, and thus, they [128] insisted that the available DIF formula on the tensile strength of plain concrete should not be simply applied for the FRC materials. The empirical formula, especially suggested to the dynamic tensile strength of FRCs, are thus collected from literature reviews and summarized in Table 2. In accordance with Yang et al. [124], the deformed (e.g., hooked and twisted) steel fibers led to the higher rate sensitivity on the tensile strength than the straight fiber due to clamping pressure and interfacial microcrack formation and, up to a certain fiber dosage (about 2.5%), the rate sensitivity increased with increasing it, similar to the trends on the compressive strength. Based on their empirical equations on the DIFs of compressive and tensile strengths [124], it was found that the tensile strength of SFRC is more sensitive to the strain-rate than its compressive strength, which is consistent with the findings of Ross [37] for plain concrete.

8. The effect of supplementary cementitious materials on the impact resistance of FRC

Alhozaimy et al. [99] investigated the effect of SCMs, such as fly ash, silica fume, and slag, on the impact resistance of FRC that includes 0.1 vol% PP fibers. Replacing a portion of cement with SCMs deteriorated the impact resistance of plain concrete. However, replacing a portion of cement in PP FRC with SCMs led to great improvement in its impact resistance, because pozzolanic action improved the bond performance of PP fibers in the cement matrix. The impact resistance at failure of PP FRC with only cement was increased by 82%, 42%, and 90% with the inclusion of fly ash, silica fume, and slag, respectively.

Toutanji et al. [92] examined the effect of silica fume on the impact resistance of PP FRC. They reported that the impact resistance of PP FRC was greatly improved with increasing amounts of silica fume, because the addition of silica fume led to better dispersion of PP fibers in the matrix. PP fibers with a length of 19 mm and a silica fume content of 10% were suggested as the optimum value. The increased brittleness of silica fume concrete was effectively mitigated by including PP fibers, and its ability to absorb kinetic energy from a drop hammer was significantly improved by adding the PP fibers. Gupta et al. [131] also reported that the impact resistance of concrete is improved by replacing fine aggregate with rubber fibers and adding silica fume.

Yan et al. [132] examined the effect of silica fume and steel fibers on the impact resistance of HSC using repeated freefalling ball tests as per ACI Committee 544. They mentioned that the impact resistance of HSC improved with the inclusion of 1.5 vol% steel fibers, but the synergetic effect of incorporating both silica fume and steel fibers led to much greater improvement, as shown in Fig. 13. In this study, 20% of the cement was replaced with silica fume. By including only steel fibers, the number of blows at first crack and failure, and the impact toughness of HSC increased by 15, 17, and 17 times, respectively, whereas by incorporating both silica fume and steel fibers, these measures increased by 22, 29, and 29 times, respectively. Thus, the addition of silica fume in the SFRC was effective in improving impact resistance. This result seems to be caused mainly by the enhanced bond strength and pullout

Table 2
– Summary of DIF models for FRCs.

Author	Type of fiber	Loading condition	Comp. strength [MPa]	Strain-rate [/s]	Fiber volume fraction [%]	Formula	Note
Lok and Zhao [12]	Steel fiber (Hooked)	Compression	91	20–100	0.6	$DIF = 1.080 + 0.017\log\dot{\varepsilon}\ \ \dot{\varepsilon} \le 20s^{-1}$ $DIF = 0.067 + 0.796\log\dot{\varepsilon}\ \ 20s^{-1} < \dot{\varepsilon} \le 100s^{-1}$	DIF = dynamic increase factor; $\dot{\varepsilon}$ = strain-rate
Ngo et al. [123]	Steel fiber (Straight)	Compression	32–160	< 300	2.0	$DIF = \left(\frac{\dot{\varepsilon}}{\dot{\varepsilon_s}}\right)^{1.026\alpha}\ \ \dot{\varepsilon} \le \dot{\varepsilon_1} s^{-1}$ $DIF = A_1\ln\dot{\varepsilon} - A_2\ \ \dot{\varepsilon_1} s^{-1} < \dot{\varepsilon} \le 300s^{-1}$	DIF = dynamic increase factor; $\dot{\varepsilon}$ = strain-rate; $\dot{\varepsilon_s}$ = static strain-rate; $\dot{\varepsilon_1} = 0.0022f_s^2 - 0.1989f_s + 46.137$; $\alpha = \frac{1}{20 + f_s/2}$; $A_1 = -0.0044f_s + 0.9866$; $A_2 = -0.0218f_s + 2.1396$; f_s = static compressive strength
Wang et al. [47]	Steel fiber (Straight) PE fiber Hybrid steel + PE fibers	Compression	around 90	10^{-4}–300	0.5, 1.0	$DIF = \left(\frac{\dot{\varepsilon}}{\dot{\varepsilon_s}}\right)^{1.026\alpha}\ \ \dot{\varepsilon} \le (30 + 23i)s^{-1}$ $DIF = \eta\left(\frac{\dot{\varepsilon}}{\dot{\varepsilon_s}}\right)^{k}\ \ (30 + 23i)s^{-1} < \dot{\varepsilon}$	DIF = dynamic increase factor; $\dot{\varepsilon}$ = strain-rate; $\dot{\varepsilon_s}$ = static strain-rate; $\alpha = \frac{1}{5 + 9 \cdot f_s/10}$; i = 0 for plain concrete and 1 for FRC; $\eta = \gamma_s(1 - 0.3392i)$; $k = (1 + 0.05i)/3$; $\gamma_s = 6.156\alpha - 2$; f_s = static compressive strength
Yang et al. [124]	Steel fiber (Straight, hooked, and twisted)	Compression	-	10^{-4}–300	0.5–6.0	$DIF = \left(\frac{\dot{\varepsilon}}{\dot{\varepsilon_s}}\right)^{1.026\alpha}\ \ \dot{\varepsilon} < \dot{\varepsilon_t} s^{-1}$ $DIF = 0.6608\beta\left(\frac{\dot{\varepsilon}}{\dot{\varepsilon_s}}\right)^{\frac{1+0.05i}{3}}\ \ \dot{\varepsilon_t} s^{-1} \le \dot{\varepsilon}$	DIF = dynamic increase factor; $\dot{\varepsilon}$ = strain-rate; $\dot{\varepsilon_s}$ = static strain-rate (3×10^{-5}/s); $\dot{\varepsilon_t}$ = transition strain-rate (34–85/s); $\alpha = \frac{1}{5 + 9 f_s/10}$; $\log\beta = 6.156K\alpha - 2.33$; K = steel fiber shape parameter (1 for straight, 1.85 for hooked, and 0.55 for twisted); i = function of fiber volume fraction; f_s = static compressive strength
Su et al. [125,135]	Ceramic fiber	Compression	56.6–65.1	20–120	0–0.3	● Plain concrete ($v_f = 0.0\%$): $DIF = 0.80582 + 0.47058\log\dot{\varepsilon}\ \ \dot{\varepsilon} \le 30s^{-1}$ $DIF = 2.28551 - 1.32826\log\dot{\varepsilon} + 0.53894\log^2\dot{\varepsilon}\ \ 30s^{-1} < \dot{\varepsilon}$ ● $v_f = 0.1\%$: $DIF = 0.67386 + 0.44832\log\dot{\varepsilon}\ \ \dot{\varepsilon} \le 30s^{-1}$ $DIF = 0.06003 + 0.64067\log\dot{\varepsilon} + 0.15321\log^2\dot{\varepsilon}\ \ 30s^{-1} < \dot{\varepsilon}$ ● $v_f = 0.2\%$: $DIF = 0.88205 + 0.33698\log\dot{\varepsilon}\ \ \dot{\varepsilon} \le 30s^{-1}$ $DIF = 6.05288 - 6.42447\log\dot{\varepsilon} + 2.20672\log^2\dot{\varepsilon}\ \ 30s^{-1} < \dot{\varepsilon}$ ● $v_f = 0.3\%$: $DIF = 0.68776 + 0.53102\log\dot{\varepsilon}\ \ \dot{\varepsilon} \le 30s^{-1}$ $DIF = 0.67773 - 0.1803\log\dot{\varepsilon} + 0.24323\log^2\dot{\varepsilon}\ \ 30s^{-1} < \dot{\varepsilon}$	v_f = fiber volume fraction; DIF = dynamic increase factor; $\dot{\varepsilon}$ = strain-rate
Hao and Hao [136]	Steel fiber (Spiral)	Compression	around 35–45	10^{-4}–200	0–1.5	● Plain concrete ($v_f = 0.0\%$): $DIF = 1.2688 + 0.0672\log\dot{\varepsilon}\ \ 10^{-4}s^{-1} \le \dot{\varepsilon} \le 64.8s^{-1}$ $DIF = 8.2551 - 8.575\log\dot{\varepsilon} + 2.6418\log^2\dot{\varepsilon}\ \ 64.8s^{-1} \le \dot{\varepsilon} \le 200s^{-1}$ ● $v_f = 0.5\%$: $DIF = 1.2716 + 0.0679og\dot{\varepsilon}\ \ 10^{-4}s^{-1} \le \dot{\varepsilon} \le 63.6s^{-1}$ $DIF = 2.4951 - 2.8505\log\dot{\varepsilon} + 1.2421\log^2\dot{\varepsilon}\ \ 63.6s^{-1} \le \dot{\varepsilon} \le 200s^{-1}$	v_f = fiber volume fraction; DIF = dynamic increase factor; $\dot{\varepsilon}$ = strain-rate

(continued on next page)

Table 2 (*continued*)

Author	Type of fiber	Loading condition	Comp. strength [MPa]	Strain-rate [/s]	Fiber volume fraction [%]	Formula	Note
Park et al. [137]	Blended steel fibers (Hooked and straight)	Tension	56, 81, 180	3.3×10^{-4}–170	2.0	• $v_f = 1.0\%$: $DIF = 1.3628 + 0.0907\log\dot{\varepsilon}\quad 10^{-4}s^{-1} \le \dot{\varepsilon} \le 58s^{-1}$ $DIF = 4.0877 - 4.7911\log\dot{\varepsilon} + 1.8921\log^2\dot{\varepsilon}\quad 58s^{-1} \le \dot{\varepsilon} \le 200s^{-1}$ • $v_f = 1.5\%$: $DIF = 1.4404 + 0.1101\log\dot{\varepsilon}\quad 10^{-4}s^{-1} \le \dot{\varepsilon} \le 50.7s^{-1}$ $DIF = 17.319 - 18.587\log\dot{\varepsilon} + 5.5039\log^2\dot{\varepsilon}\quad 50.7s^{-1} \le \dot{\varepsilon} \le 200s^{-1}$ $DIF = \left(\frac{\dot{\varepsilon}}{\dot{\varepsilon_s}}\right)^{\delta}\quad \dot{\varepsilon} < 25s^{-1} DIF = \beta\left(\frac{\dot{\varepsilon}}{\dot{\varepsilon_s}}\right)^{\mu}\quad 25s^{-1} \le \dot{\varepsilon}$	DIF = dynamic increase factor; $\dot{\varepsilon}$ = strain-rate; $\delta = 0.017 - 2722 \times \left(\frac{f_s}{10}\right)^{-7.33}$; $\log\beta = -0.007082 \times f_s - 2.08$; $\mu = 0.1208 f_s^{0.2622}$; $\dot{\varepsilon_s} = 1 \times 10^{-6}s^{-1}$; f_s = static compressive strength
Yang et al. [124]	Steel fiber (Straight, hooked, and twisted)	Tension	56–190	-	1.0–3.0	$DIF = \left(\frac{\dot{\varepsilon}}{\dot{\varepsilon_s}}\right)^{k\delta}\quad \dot{\varepsilon} \le \dot{\varepsilon_t} s^{-1} DIF = m\beta\left(\frac{\dot{\varepsilon}}{\dot{\varepsilon_s}}\right)^{\frac{1}{3}}\quad \dot{\varepsilon_t} s^{-1} < \dot{\varepsilon}$	DIF = dynamic increase factor; $\dot{\varepsilon}$ = strain-rate; $\dot{\varepsilon_s}$ = static strain-rate (1×10^{-6}/s); $\dot{\varepsilon_t}$ = transition strain-rate (0.65–18/s); $\delta = \frac{1}{1 + 8 \cdot f_s / 10}$; $\log\beta = 7K\alpha - 2.141$; K = steel fiber shape parameter (0.8 for straight, 0.95 for hooked, and 1.3 for twisted); m = a parameter describing fiber volume fraction (0.54–1.25); f_s = static compressive strength
Xu et al. [128]	Steel fiber (Hooked and spiral)	Tension	-	-	1.0–2.0	$DIF = 1.0345 + 0.0095\dot{\varepsilon}\quad \dot{\varepsilon} \le 30s^{-1} DIF = 0.2981 - 0.0436\dot{\varepsilon} + 0.00004\dot{\varepsilon}^2\quad 30s^{-1} < \dot{\varepsilon}$	DIF = dynamic increase factor; $\dot{\varepsilon}$ = strain-rate
Hao and Hao [71]	Steel fiber (Spiral)	Tension	> 33	2–20	0–1.5	• Plain concrete ($v_f = 0.0\%$): $DIF = 0.7085 + 3.0701\log\dot{\varepsilon}\quad 2s^{-1} \le \dot{\varepsilon} \le 20s^{-1}$ • $v_f = 0.5\%$: $DIF = 1.3493 + 3.4471\log\dot{\varepsilon}\quad 2s^{-1} \le \dot{\varepsilon} \le 20s^{-1}$ • $v_f = 1.0\%$: $DIF = 2.2996 + 3.1296\log\dot{\varepsilon}\quad 2s^{-1} \le \dot{\varepsilon} \le 20s^{-1}$ • $v_f = 1.5\%$: $DIF = 2.3491 + 4.0106\log\dot{\varepsilon}\quad 2s^{-1} \le \dot{\varepsilon} \le 20s^{-1}$	DIF = dynamic increase factor; $\dot{\varepsilon}$ = strain-rate
Thomas and Sorensen [138]	Steel fiber (straight, hooked, and twisted) PE fiber	Tension	150	10^{-6}–100	0–6.0	$DIF = \left(\frac{\dot{\varepsilon}}{\dot{\varepsilon_s}}\right)^{\delta}\quad \dot{\varepsilon} \le 10s^{-1} DIF = \beta\left(\frac{\dot{\varepsilon}}{\dot{\varepsilon_s}}\right)^{\frac{3}{4}}\quad 10s^{-1} < \dot{\varepsilon}$	DIF = dynamic increase factor; $\dot{\varepsilon}$ = strain-rate; $\dot{\varepsilon_s} = 1 \times 10^{-6}s^{-1}$; $\delta = \frac{1}{1 + 8 \cdot f_s / 10}$; $\log\beta = 7\delta - 5.25$; f_s = static compressive strength

[Note] PE = polyethylene.

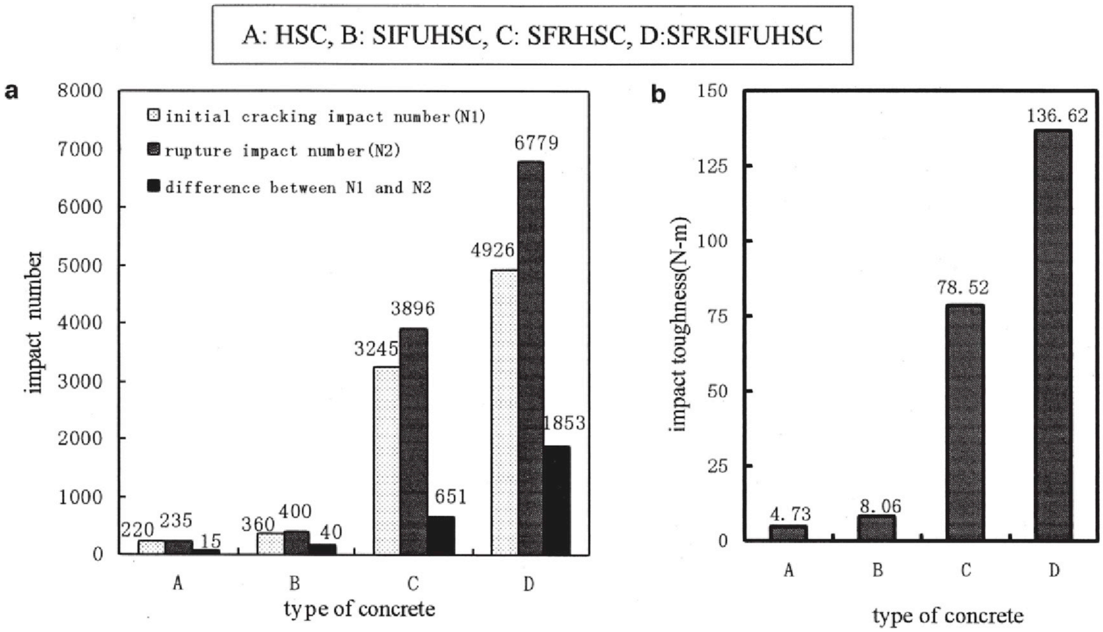

Fig. 13. Impact resistance of high strength concretes with and without silica fume and steel fibers; (a) number of blows, (b) impact toughness (HSC = high strength concrete, SIFUHSC = silica fume HSC, SFRHSC = steel fiber reinforced HSC, SFRSIFUHSC = HSC with silica fume and steel fibers) [132].

energy of the steel fibers. According to pullout test results from Chan and Chu [133], the bond strength and pullout energy of steel fibers embedded in an ultra-high-strength cement matrix increased as the amount of silica fume was increased up to 30%. For example, the pullout energy increased by nearly 100% by replacing 30% of the cement with silica fume.

Siddique [134] studied the impact resistance of concrete with high volumes of class F fly ash and natural san fibers, a subset of natural bast fibers. Portland cement was replaced with 35%, 45%, or 55% of class F fly ash, and san fibers were incorporated as 0.25%, 0.5%, or 0.75% of the mixture. The addition of san fibers improves the impact resistance of plain fly ash concrete; the improvement increased with the fiber content. However, the best impact resistance was achieved by concrete with 35% fly ash, regardless of the fiber content; impact resistance decreases with increasing amounts of fly ash. Thus, high volumes of fly ash are not effective in improving the impact resistance of concrete with natural san fibers.

9. Conclusion

This paper comprehensively reviewed the impact resistance of ordinary FRC with various fiber types. Based on literature reviews, several important findings were obtained, and the following conclusions could be drawn from the above discussions.

1) The strain-rate sensitivity of FRCs differs according to loading condition, matrix strength, and saturation. Tensile impacts lead to the highest rate sensitivity, followed by flexural and compressive impacts. Matrix strength also affects the strain-rate sensitivity of FRC: higher strength FRC is less sensitive to strain-rate than the lower strength FRC. Lastly, saturated concrete exhibits increased strain-rate sensitivity compared with dry concrete.
2) The size effect on the flexural toughness of FRCs becomes more pronounced at higher impact intensities.
3) The pullout resistance of straight steel fiber, which is resisted by only its frictional component, is almost insensitive to the loading rate. Conversely, the pullout resistance of deformed steel and PP fibers greatly improves with increasing loading rate. In the case of deformed steel fibers, once a fiber is fractured, pullout resistance decreases at higher loading rate. These results indicate that the strength of fibers must be properly designed to prevent their fracture under impact.
4) Higher rate sensitivity on the bond strength is observed in the multiple steel fibers than the single steel fiber. However, increasing the number of steel fibers generally decreases the average bond strengths under impact load.
5) In contrast with the single-fiber pullout impact test results, the SFRC including straight steel fibers exhibits almost a threefold increase of flexural strength at the strain-rate increased from 0.5×10^{-5}/s to 1.2/s, due to their inclination.
6) Impact resistance, including both the strength and energy absorption capacity, of plain concrete greatly improves with the inclusion of deformed steel fibers and increasing their amount under compression, tension, and flexure. Hooked steel fibers are most effective in improving impact resistance, followed by crimped, flat-end, and twin-cone steel fibers. However, the difference in the impact resistances between SFRC with hooked and crimped steel fibers is minor compared with that between SFRC with hooked and flat-end (or twin-cone) steel fibers.
7) Hooked steel fiber with a higher aspect ratio is more efficient in improving FRC's compressive toughness under impact. In addition, FRCs including PE and steel fibers are less sensitive to strain-rate on compressive strength and toughness compared with plain concrete.
8) The addition of steel fibers effectively decreases the impact damage (i.e., the size of craters and penetration depth) of concrete panels under projectile impact, and also, it is more effective in reducing crater area and scabbing than penetration depth.
9) The impact resistance of concrete under flexure and compression improves with the inclusion of PP and PVA fibers. Crimped PP fibers are more effective in improving the impact resistance of concrete than straight ones, and longer PP fibers give better impact resistance than shorter ones. Compared to PP fibers, nylon fibers more effectively improve the impact resistance of concrete, whereas PVA fibers do so less effectively. Since PVA fibers provide higher impact resistance than PO fibers, the impact resistance of polymeric and nylon FRCs by fiber type in descending order is nylon, PP, PVA, and PO.
10) Carbon and basalt fibers enhance the impact resistance of concrete. However, the strengthening effect of basalt fiber is more significant compared to that of carbon fiber; the effectiveness of adding carbon

fiber is especially diminished at very high loading rates, causing the fiber fracture.

11) The impact resistance of single SFRC is enhanced by replacing a portion of steel fibers with PP, palm, or synthetic fibers, to form a hybrid FRC. However, since single steel fibers generally provide better impact resistance than single PP, palm, and synthetic fibers, this enhancement is only obtained by replacing a small amount of steel fiber. The optimum volume proportion of steel and PP fibers is suggested to be 2:1.
12) Among natural FRCs, the addition of jute and coir fibers is slightly more effective in improving the impact resistance of concrete compared with that of bamboo fibers.
13) SFRC that includes deformed steel fibers generally exhibits better impact resistance than polymeric (i.e., PP, PO, PVA, and PE) and carbon FRCs. However, the difference in impact resistance between concretes with deformed steel and polymeric fibers decreases with greater impact intensities, due to the deformed steel fiber's higher possibility of fracture at very high loading rates.
14) Glass fiber is more effective than PP fiber in improving the resistance to repeated impact loads. However, since the higher rate sensitivity of PP fiber on its tensile strength than that of glass fiber, the PP FRC has a higher energy absorption capacity than the glass FRC.
15) Significant improvement in the impact resistance of PP FRC can be obtained by replacing a portion of cement with SCMs such as fly ash, silica fume, or slag. The use of silica fume significantly improves the impact resistance of SFRC, whereas a high volume of fly ash deteriorates the impact resistance of concrete reinforced with natural san fibers.

Acknowledgements

This work was supported by the National Research Foundation of Korea (NRF) grant funded by the Korea government (MSIT) (No. 2017R1C1B2007589).

References

[1] A. Bentur, S. Mindess, Fibre Reinforced Cementitious Composites, CRC Press, 2006.
[2] D.Y. Yoo, U. Gohil, T. Gries, Y.S. Yoon, Comparative low-velocity impact response of textile-reinforced concrete and steel-fiber-reinforced concrete beams, J. Compos. Mater. 50 (17) (2016) 2421–2431.
[3] D.Y. Yoo, Y.S. Yoon, Influence of steel fibers and fiber-reinforced polymers on the impact resistance of one-way concrete slabs, J. Compos. Mater. 48 (6) (2014) 695–706.
[4] A.M. Brandt, Fibre reinforced cement-based (FRC) composites after over 40 years of development in building and civil engineering, Compos. Struct. 86 (1) (2008) 3–9.
[5] D.J. Kim, K. Wille, S. El-Tawil, A.E. Naaman, Testing of cementitious materials under high-strain-rate tensile loading using elastic strain energy, J. Eng. Mech. 137 (2011) 1–8.
[6] V. Bindiganavile, N. Banthia, Polymer and steel fiber-reinforced cementitious composites under impact loading—Part 1: bond-slip, ACI Mater. J. 98 (1) (2001) 10–16.
[7] Y.S. Tai, S. El-Tawil, T.H. Chung, Performance of deformed steel fibers embedded in ultra-high performance concrete subjected to various pullout rates, Cement Concr. Res. 89 (2016) 1–13.
[8] D.Y. Yoo, S. Kim, Comparative pullout behavior of half-hooked and commercial steel fibers embedded in UHPC under static and impact loads, Cem. Concr. Compos. 97 (2019) 89–106.
[9] JSCE, Recommendations for Design and Construction of Ultra-high Strength Fiber Reinforced Concrete Structures (Draft), Japan Society of Civil Engineers, Tokyo, Japan, 2004.
[10] P.H. Bischoff, S.H. Perry, Compressive behaviour of concrete at high strain rates, Mater. Struct. 24 (6) (1991) 425–450.
[11] S. Hentz, F.V. Donzé, L. Daudeville, Discrete element modelling of concrete submitted to dynamic loading at high strain rates, Comput. Struct. 82 (29–30) (2004) 2509–2524.
[12] T.S. Lok, P.J. Zhao, Impact response of steel fiber-reinforced concrete using a split Hopkinson pressure bar, J. Mater. Civ. Eng. 16 (1) (2004) 54–59.
[13] W. Li, J. Xu, Impact characterization of basalt fiber reinforced geopolymeric concrete using a 100-mm-diameter split Hopkinson pressure bar, Mater. Sci. Eng. A 513 (2009) 145–153.
[14] D.L. Grote, S.W. Park, M. Zhou, Dynamic behavior of concrete at high strain rates and pressures: I. experimental characterization, Int. J. Impact Eng. 25 (9) (2001) 869–886.
[15] Q.M. Li, H. Meng, About the dynamic strength enhancement of concrete-like materials in a split Hopkinson pressure bar test, Int. J. Solids Struct. 40 (2) (2003) 343–360.
[16] N. Banthia, P. Gupta, C. Yan, Impact resistance of fiber reinforced wet-mix shotcrete–Part 2: plate tests, Mater. Struct. 32 (9) (1999) 643–650.
[17] A. Bentur, S. Mindess, N. Banthia, The behaviour of concrete under impact loading: experimental procedures and method of analysis, Mater. Struct. 19 (5) (1986) 371–378.
[18] D.Y. Yoo, N. Banthia, S.T. Kang, Y.S. Yoon, Effect of fiber orientation on the rate-dependent flexural behavior of ultra-high-performance fiber-reinforced concrete, Compos. Struct. 157 (2016) 62–70.
[19] A.A. Nia, M. Hedayatian, M. Nili, V.A. Sabet, An experimental and numerical study on how steel and polypropylene fibers affect the impact resistance in fiber-reinforced concrete, Int. J. Impact Eng. 46 (2012) 62–73.
[20] N. Banthia, K. Chokri, Y. Ohama, S. Mindess, Fiber-reinforced cement based composites under tensile impact, Adv. Cem. Base Mater. 1 (3) (1994) 131–141.
[21] N. Banthia, S. Mindess, J.E. Trorrier, Impact resistance of steel fiber reinforced concrete, ACI Mater. J. 93 (1996) 472–479.
[22] S. Pyo, S. El-Tawil, Capturing the strain hardening and softening responses of cementitious composites subjected to impact loading, Constr. Build. Mater. 81 (2015) 276–283.
[23] T.K. Tran, D.J. Kim, Strain energy impact test machine (SEFIM), J. Adv. Concr. Technol. 10 (2012) 126–136.
[24] T.H. Almusallam, N.A. Siddiqui, R.A. Iqbal, H. Abbas, Response of hybrid-fiber reinforced concrete slabs to hard projectile Impact, Int. J. Impact Eng. 58 (2013) 17–30.
[25] D.Y. Yoo, N. Banthia, Size-dependent impact resistance of ultra-high-performance fiber-reinforced concrete beams, Constr. Build. Mater. 142 (2017) 363–375.
[26] N. Banthia, S. Mindess, A. Bentur, M. Pigeon, Impact testing of concrete using a drop-weight impact machine, Exp. Mech. 29 (1) (1989) 63–69.
[27] X.X. Zhang, A.A. Elazim, G. Ruiz, R.C. Yu, Fracture behaviour of steel fibre-reinforced concrete at a wide range of loading rates, Int. J. Impact Eng. 71 (2014) 89–96.
[28] S.M. Soleimani, N. Banthia, A novel drop weight impact setup for testing reinforced concrete beams, Exp. Tech. 38 (3) (2014) 72–79.
[29] D.Y. Yoo, N. Banthia, Y.S. Yoon, Impact resistance of reinforced ultra-high-performance concrete beams with different steel fibers, ACI Struct. J. 114 (1) (2017) 113–124.
[30] D.Y. Yoo, Y.S. Yoon, N. Banthia, Flexural response of steel-fiber-reinforced concrete beams: effects of strength, fiber content, and strain-rate, Cement Concr. Compos. 64 (2015) 84–92.
[31] V. Dey, A. Bonakdar, B. Mobasher, Low-velocity flexural impact response of fiber-reinforced aerated concrete, Cement Concr. Compos. 49 (2014) 100–110.
[32] V. Bindiganavile, N. Banthia, Polymer and steel fiber-reinforced cementitious composites under impact loading–Part 2: flexural toughness, ACI Mater. J. 98 (1) (2001) 17–24.
[33] N. Banthia, Enhancing Impact and Blast Resistance of Concrete with Fiber Reinforcement. Resilience of Cities to Terrorist and Other Threats. NATO Science for Peace and Security Series C: Environmental Security, North Atlantic Treaty Organization, Moscow, 2008, pp. 171–187.
[34] V. Bindiganavile, N. Banthia, B. Aarup, Impact response of ultra-high-strength fiber-reinforced cement composite, ACI Mater. J. 99 (6) (2002) 543–548.
[35] V. Bindiganavile, N. Banthia, Generating dynamic crack growth resistance curves for fiber-reinforced concrete, Exp. Mech. 45 (2) (2005) 112–122.
[36] S. Mindess, J.F. Young, D. Darwin, Concrete, second ed., Pearson Education Inc., New Jersey, 2003.
[37] C.A. Ross, Review of strain-rate effects in materials, Structures under Extreme Loading Conditions, ASME Pressure Vessels and Piping Conference, 1997, pp. 255–262.
[38] W. Suaris, S.P. Shah, Strain-rate effects in fibre-reinforced concrete subjected to impact and impulsive loading, Compos 13 (2) (1982) 153–159.
[39] N. Banthia, M. Pigeon, Dynamic behavior of concrete and its fiber reinforced composites: a review and future research needs, in: P.S. Bulson (Ed.), Structures under Shock and Impact, Proceeding of the 1st International Conference, Cambridge, Massachusetts. USA, July 1989.
[40] A. Bentur, S. Mindess, N. Banthia, Behavior of Reinforced Concrete under Impact: the Effect of Concrete Strength, Society for Experimental Mechanics, Inc., Bethel, Conn., 1987, pp. 449–458.
[41] N. Banthia, Impact resistance of HPFRCC, International RILEM Workshop on High Performance Fiber Reinforced Composites (HPFRCC) in Structural Applications, Honolulu, Hawaii, USA, 2005, pp. 479–488.
[42] P.H. Bischoff, S.H. Perry, Impact behavior of plain concrete loaded in uniaxial compression, J. Eng. Mech. 121 (6) (1995) 685–693.
[43] J. Sercombe, F.J. Ulm, F. Toutlemonde, Viscous hardening plasticity for concrete in high rate dynamics, J. Eng. Mech. 124 (9) (1998) 1050–1057.
[44] N. Banthia, C. Yan, K. Sakai, Impact resistance of fiber reinforced concrete at subnormal temperatures, Cement Concr. Compos. 20 (5) (1998) 393–404.
[45] Y. Qian, S.R. Swanson, R.J. Nuismer, R.B. Bucinell, An experimental study of scaling rules for impact damage in fiber composites, J. Compos. Mater. 24 (5) (1990) 559–570.
[46] J. Morton, Scaling of impact-loaded carbon-fiber composites, AIAA J. 26 (8) (1988) 989–994.
[47] S. Wang, M.H. Zhang, S.T. Quek, Effect of high strain rate loading on compressive

behaviour of fibre-reinforced high-strength concrete, Mag. Concr. Res. 63 (11) (2011) 813–827.
[48] ACI Committee 446, Report on Dynamic Fracture of Concrete, American Concrete Institute, Farmington Hills, Michigan, 2004 Report 446.4R-04.
[49] N. Banthia, V. Bindiganavile, S. Mindess, Impact resistance of fiber reinforced concrete: a progress report, Proceedings of High Performance Fiber Reinforced Concrete 4, RILEM, Cachan Cedex, France, 2003, pp. 117–131 2003.
[50] B. Mobasher, C. Ouyang, S.P. Shah, Modeling of fiber toughening in cementitious materials using an R-curve approach, Int. J. Fract. 50 (3) (1991) 199–219.
[51] A. Hillerborg, Analysis of fracture by means of the fictitious crack model, particularly for fibre reinforced concrete, Cement Concr. Compos. 2 (4) (1980) 177–184.
[52] S. Mindess, F.V. Lawrence, C.E. Kesler, The J-integral as a fracture criterion for fiber reinforced concrete, Cement Concr. Res. 7 (6) (1977) 731–742.
[53] V. Bindiganavile, Dynamic Fracture Toughness of Fiber Reinforced Concrete, Doctoral dissertation, University of British Columbia, British Columbia, Canada, 2003, p. 231.
[54] S. Mindess, N. Banthia, A. Ritter, J. Skalny, Crack development in cementitious materials under impact loading, in: S. Mindess, S.P. Shah (Eds.), Proceedings of the Materials Research Society Symposium, Cement Based Composites: Strain Rate Effects on Fracture, vol. 64, 1986, pp. 217–223 Boston, MA.
[55] U.N. Gokoz, A.E. Naaman, Effect of strain-rate on the pull-out behaviour of fibres in mortar, Int. J. Cem. Compos. Lightweight Concr. 3 (3) (1981) 187–202.
[56] E. Vos, H.W. Reinhardt, Bond Resistance of Deformed Bars, Plain Bars and Strands under Impact Loading. Report No. 5-80-6, Department of Civil Engineering, Delft University of Technology, The Netherlands, Sept., 1980.
[57] A.E. Naaman, Fiber reinforced concrete under dynamic loading, ACI Spec. Publ. 81 (1984) 169–186.
[58] A. Pacios, C. Ouyang, S.P. Shah, Rate effect on interfacial response between fibres and matrix, Mater. Struct. 28 (2) (1995) 83–91.
[59] N. Banthia, J.F. Trottier, Deformed steel fiber—cementitious matrix bond under impact, Cement Concr. Res. 21 (1) (1991) 158–168.
[60] A.E. Naaman, V.S. Gopalaratnam, Impact properties of steel fibre reinforced concrete in bending, Int. J. Cem. Compos. Lightweight Concr. 5 (4) (1983) 225–233.
[61] K.C.G. Ong, M. Basheerkhan, P. Paramasivam, Resistance of fibre concrete slabs to low velocity projectile impact, Cement Concr. Compos. 21 (5) (1999) 391–401.
[62] N. Wang, S. Mindess, K. Ko, Fibre reinforced concrete beams under impact loading, Cement Concr. Res. 26 (3) (1996) 363–376.
[63] H.T. Wang, L.C. Wang, Experimental study on static and dynamic mechanical properties of steel fiber reinforced lightweight aggregate concrete, Constr. Build. Mater. 38 (2013) 1146–1151.
[64] N. Banthia, P. Gupta, C. Yan, Impact resistance of fiber reinforced wet-mix shotcrete - Part I: beam tests, Mater. Struct. 32 (8) (1999) 563–570.
[65] P. Gupta, N. Banthia, C. Yan, Fiber reinforced wet-mix shotcrete under impact, J. Mater. Civ. Eng. 12 (1) (2000) 81–90.
[66] G. Murali, A.S. Santhi, G.M. Ganesh, Impact resistance and strength reliability of fiber reinforced concrete using two parameter weibull distribution, ARPN J. Eng. Appl. Sci. 9 (4) (2014) 554–559.
[67] M. Nili, V. Afroughsabet, Combined effect of silica fume and steel fibers on the impact resistance and mechanical properties of concrete, Int. J. Impact Eng. 37 (8) (2010) 879–886.
[68] P. Ramadoss, K. Nagamani, Impact characteristics of high-performance steel fiber reinforced concrete under repeated dynamic loading, Int. J. Civ. Eng. 12 (4) (2014) 513–520.
[69] H.S. Armelin, N. Banthia, Predicting the flexural postcracking performance of steel fiber reinforced concrete from the pullout of single fibers, ACI Mater. J. 94 (1997) 18–31.
[70] N. Banthia, A study of some factors affecting the fiber–matrix bond in steel fiber reinforced concrete, Can. J. Civ. Eng. 17 (4) (1990) 610–620.
[71] Y. Hao, H. Hao, Mechanical properties and behaviour of concrete reinforced with spiral-shaped steel fibres under dynamic splitting tension, Mag. Concr. Res. 68 (21) (2016) 1110–1121.
[72] H. Hao, Y. Hao, Performance of spiral-shaped steel fibre reinforced concrete structure under static and dynamic loads, International Conference on Performance-Based and Life-Cycle Structural Engineering, The University of Queensland, Australia, 2015, pp. 58–68.
[73] M. Pająk, Dynamic response of SFRC under different strain rates–an overview of test results, 7th International Conference Analytical Models and New Concepts in Concrete and Masonry Structures, Kraków, Poland, 2011.
[74] S. Wang, M.H. Zhang, S.T. Quek, Mechanical behavior of fiber-reinforced high-strength concrete subjected to high strain-rate compressive loading, Constr. Build. Mater. 31 (2012) 1–11.
[75] S.S. Wang, M.H. Zhang, S.T. Quek, Compressive behavior of plain and fiber-reinforced high-strength concrete subjected to high strain rate loading, Appl. Mech. Mater. 82 (2011) 57–62.
[76] Z.L. Wang, Y.S. Liu, R.F. Shen, Stress–strain relationship of steel fiber-reinforced concrete under dynamic compression, Constr. Build. Mater. 22 (5) (2008) 811–819.
[77] Z.L. Wang, Z.M. Shi, J.G. Wang, On the strength and toughness properties of SFRC under static-dynamic compression, Compos. B Eng. 42 (5) (2011) 1285–1290.
[78] T.C. Yet, R. Hamid, M. Kasmuri, Dynamic stress-strain behaviour of steel fiber reinforced high-performance concrete with fly ash, Adv. Civ. Eng. 2012 (2012) 907431.
[79] W.F. Brace, A.H. Jones, Comparison of uniaxial deformation in shock and static loading of three rocks, J. Geophys. Res. 76 (20) (1971) 4913–4921.
[80] P.H. Bischoff, S.H. Perry, Compressive strain rate effects of concrete, Materials Research Society Symposia Proceedings vol. 64, Cambridge University Press, 1985, p. 151.
[81] CEB Comité, Euro-International du Béton. CEB-FIP, Model Code 1990, Thomas Telford, London, 1993.
[82] Z. Xu, H. Hao, H.N. Li, Mesoscale modelling of fibre reinforced concrete material under compressive impact loading, Constr. Build. Mater. 26 (1) (2012) 274–288.
[83] A.H.H. Al-Masoodi, A. Kawan, M. Kasmuri, R. Hamid, M.N.N. Khan, Static and dynamic properties of concrete with different types and shapes of fibrous reinforcement, Constr. Build. Mater. 104 (2016) 247–262.
[84] K. Marar, Ö. Eren, T. Celik, Relationship between impact energy and compression toughness energy of high-strength fiber-reinforced concrete, Mater. Lett. 47 (4) (2001) 297–304.
[85] K. Fujikake, K. Uebayashi, T. Ohno, Y. Shimoyama, M. Katagiri, Dynamic properties of steel fiber reinforced mortar under high-rates of loadings and triaxial stress states, Proceedings of the 7th International Conference on Structures under Shock and Impact, Montreal, 2002, pp. 437–446.
[86] T.L. Teng, Y.A. Chu, F.A. Chang, B.C. Shen, D.S. Cheng, Development and validation of numerical model of steel fiber reinforced concrete for high-velocity impact, Comput. Mater. Sci. 42 (1) (2008) 90–99.
[87] E.M. Almansa, M.F. Cánovas, Behaviour of normal and steel fiber-reinforced concrete under impact of small projectiles, Cement Concr. Res. 29 (11) (1999) 1807–1814.
[88] A.N. Dancygier, A. Katz, D. Benamou, D.Z. Yankelevsky, Resistance of double-layer reinforced HPC barriers to projectile impact, Int. J. Impact Eng. 67 (2014) 39–51.
[89] M.H. Zhang, V.P.W. Shim, G. Lu, C.W. Chew, Resistance of high-strength concrete to projectile impact, Int. J. Impact Eng. 31 (7) (2005) 825–841.
[90] X. Luo, W. Sun, S.Y. Chan, Characteristics of high-performance steel fiber-reinforced concrete subject to high velocity impact, Cement Concr. Res. 30 (6) (2000) 907–914.
[91] X. Luo, W. Sun, S.Y. Chan, Steel fiber reinforced high-performance concrete: a study on the mechanical properties and resistance against impact, Mater. Struct. 34 (3) (2001) 144–149.
[92] H. Toutanji, S. McNeil, Z. Bayasi, Chloride permeability and impact resistance of polypropylene-fiber-reinforced silica fume concrete, Cement Concr. Res. 28 (7) (1998) 961–968.
[93] M. Nili, V. Afroughsabet, The effects of silica fume and polypropylene fibers on the impact resistance and mechanical properties of concrete, Constr. Build. Mater. 24 (6) (2010) 927–933.
[94] G.D. Manolis, P.J. Gareis, A.D. Tsonos, J.A. Neal, Dynamic properties of polypropylene fiber-reinforced concrete slabs, Cement Concr. Compos. 19 (4) (1997) 341–349.
[95] P.S. Song, S. Hwang, B.C. Sheu, Strength properties of nylon-and polypropylene-fiber-reinforced concretes, Cement Concr. Res. 35 (8) (2005) 1546–1550.
[96] P. Soroushian, J. Plasencia, S. Ravanbakhsh, Assessment of reinforcing effects of recycled plastic and paper in concrete, ACI Mater. J. 100 (3) (2003) 203–207.
[97] S. Mindess, G. Vondran, Properties of concrete reinforced with fibrillated polypropylene fibres under impact loading, Cement Concr. Res. 18 (1) (1988) 109–115.
[98] S. Mindess, N. Banthia, C. Yan, The fracture toughness of concrete under impact loading, Cement Concr. Res. 17 (2) (1987) 231–241.
[99] A.M. Alhozaimy, P. Soroushian, F. Mirza, Mechanical properties of polypropylene fiber reinforced concrete and the effects of pozzolanic materials, Cement Concr. Compos. 18 (2) (1996) 85–92.
[100] S. Mindness, A. Bentur, C. Yan, G. Vondran, Impact resistance of concrete containing both conventional steel reinforcement and fibrillated polypropylene fibers, ACI Mater. J. 86 (6) (1989) 545–549.
[101] B. Xu, H.A. Toutanji, J. Gilbert, Impact resistance of poly (vinyl alcohol) fiber reinforced high-performance organic aggregate cementitious material, Cement Concr. Res. 40 (2) (2010) 347–351.
[102] Z. Yunsheng, S. Wei, L. Zongjin, Z. Xiangming, C. Chungkong, Impact properties of geopolymer based extrudates incorporated with fly ash and PVA short fiber, Constr. Build. Mater. 22 (3) (2008) 370–383.
[103] D. Foti, F. Paparella, Impact behavior of structural elements in concrete reinforced with PET grids, Mech. Res. Commun. 57 (2014) 57–66.
[104] N. Banthia, Y. Ohama, Dynamic tensile fracture of carbon fiber reinforced cements, Proceedings of International Conference on Fiber Reinforced Cements, Cardiff, England, 1989, pp. 251–260.
[105] Y. Ohama, M. Amano, M. Endo, Properties of carbon fiber reinforced cement with silica fume, Concr. Int. 7 (3) (1985) 58–62.
[106] Z.S. Tabatabaei, J.S. Volz, J. Baird, B.P. Gliha, D.I. Keener, Experimental and numerical analyses of long carbon fiber reinforced concrete panels exposed to blast loading, Int. J. Impact Eng. 57 (2013) 70–80.
[107] V.T. Giner, F.J. Baeza, S. Ivorra, E. Zornoza, O. Galao, Effect of steel and carbon fiber additions on the dynamic properties of concrete containing silica fume, Mater. Des. 34 (2012) 332–339.
[108] W. Li, J. Xu, Mechanical properties of basalt fiber reinforced geopolymeric concrete under impact loading, Mater. Sci. Eng. A 505 (1) (2009) 178–186.
[109] W.M. Li, J.Y. Xu, L.J. Shen, Q. Li, Dynamic mechanical properties of basalt fiber reinforced concrete using a split Hopkinson pressure bar, Acta Mater. Compos. Sin. 25 (2008) 135–142.
[110] H.S. Ramaswamy, B.M. Ahuja, S. Krishnamoorthy, Behaviour of concrete reinforced with jute, coir and bamboo fibres, Int. J. Cem. Compos. Lightweight Concr. 5 (1) (1983) 3–13.
[111] F. de Andrade Silva, D. Zhu, B. Mobasher, R.D. Toledo Filho, Impact behavior of

sisal fiber cement composites under flexural load, ACI Mater. J. 108 (2) (2011) 168–177.
[112] D. Zhu, M. Gencoglu, B. Mobasher, Low velocity flexural impact behavior of AR glass fabric reinforced cement composites, Cement Concr. Compos. 31 (6) (2009) 379–387.
[113] P.S. Song, J.C. Wu, S. Hwang, B.C. Sheu, Statistical analysis of impact strength and strength reliability of steel–polypropylene hybrid fiber-reinforced concrete, Constr. Build. Mater. 19 (1) (2005) 1–9.
[114] P. Wang, Z. Huang, J. Jiang, Y. Wu, Performance of hybrid fiber reinforced concrete with steel fibers and polypropylene fibers, Civil Engineering and Urban Planning, 2012, pp. 458–461.
[115] S.T. Yildirim, C.E. Ekinci, F. Findik, Properties of hybrid fiber reinforced concrete under repeated impact loads, Russ. J. Nondestruct. Test. 46 (7) (2010) 538–546.
[116] K.H. Mo, S.P. Yap, U.J. Alengaram, M.Z. Jumaat, C.H. Bu, Impact resistance of hybrid fibre-reinforced oil palm shell concrete, Constr. Build. Mater. 50 (2014) 499–507.
[117] N. Banthia, N. Nandakumar, Crack growth resistance of hybrid fiber reinforced cement composites, Cement Concr. Compos. 25 (1) (2003) 3–9.
[118] T.H. Almusallam, A.A. Abadel, Y.A. Al-Salloum, N.A. Siddiqui, H. Abbas, Effectiveness of hybrid-fibers in improving the impact resistance of RC slabs, Int. J. Impact Eng. 81 (2015) 61–73.
[119] E.T. Dawood, M. Ramli, Mechanical properties of high strength flowing concrete with hybrid fibers, Constr. Build. Mater. 28 (1) (2012) 193–200.
[120] ACI Committee 544, Design considerations for steel fiber reinforced concrete, ACI 544.4R-88, Farmington Hills: American Concrete Institute, 1988.
[121] W. Suaris, S.P. Shah, Properties of concrete subjected to impact, J. Struct. Eng. 109 (7) (1983) 1727–1741.
[122] A.E. Naaman, S.R. Shah, Pull-out mechanism in steel fiber-reinforced concrete, J. Struct. Div. 102 (1976) 1537–1548.
[123] T. Ngo, P. Mendis, T. Krauthammer, Behavior of ultrahigh-strength prestressed concrete panels subjected to blast loading, J. Struct. Eng. 133 (11) (2007) 1582–1590.
[124] L. Yang, X. Lin, R.J. Gravina, Evaluation of dynamic increase factor models for steel fibre reinforced concrete, Constr. Build. Mater. 190 (2018) 632–644.
[125] H. Su, J. Xu, W. Ren, Mechanical properties of ceramic fiber-reinforced concrete under quasi-static and dynamic compression, Mater. Des. 57 (2014) 426–434.
[126] L.J. Malvar, C.A. Ross, Review of strain rate effects for concrete in tension, ACI Mater. J. 95 (6) (1998) 735–739.
[127] H. Othman, H. Marzouk, Strain rate sensitivity of fiber-reinforced cementitious composites, ACI Mater. J. 113 (2) (2016) 143–150.
[128] Z. Xu, H. Hao, H.N. Li, Mesoscale modelling of dynamic tensile behaviour of fibre reinforced concrete with spiral fibres, Cement Concr. Res. 42 (11) (2012) 1475–1493.
[129] S.P. Shah, Concrete and fiber reinforced concrete subjected to impact loading, Mater. Res. Soc. Symp. Proc. 64 (1986) 181–201.
[130] Z. Wang, N. Zhou, J. Wang, Using Hopkinson pressure bar to perform dynamic tensile tests on SFRC at medium strain rates, Mag. Concr. Res. 64 (8) (2012) 657–664.
[131] T. Gupta, R.K. Sharma, S. Chaudhary, Impact resistance of concrete containing waste rubber fiber and silica fume, Int. J. Impact Eng. 83 (2015) 76–87.
[132] H. Yan, W. Sun, H. Chen, The effect of silica fume and steel fiber on the dynamic mechanical performance of high-strength concrete, Cement Concr. Res. 29 (3) (1999) 423–426.
[133] Y.W. Chan, S.H. Chu, Effect of silica fume on steel fiber bond characteristics in reactive powder concrete, Cement Concr. Res. 4 (7) (2004) 1167–1172.
[134] R. Siddique, Properties of concrete incorporating high volumes of class F fly ash and san fibers, Cement Concr. Res. 34 (1) (2004) 37–42.
[135] H. Su, J. Xu, Dynamic compressive behavior of ceramic fiber reinforced concrete under impact load, Constr. Build. Mater. 45 (2013) 306–313.
[136] Y. Hao, H. Hao, Dynamic compressive behaviour of spiral steel fibre reinforced concrete in split Hopkinson pressure bar tests, Constr. Build. Mater. 48 (2013) 521–532.
[137] J.K. Park, S.W. Kim, D.J. Kim, Matrix-strength-dependent strain-rate sensitivity of strain-hardening fiber-reinforced cementitious composites under tensile impact, Compos. Struct. 162 (2017) 313–324.
[138] R.J. Thomas, A.D. Sorensen, Review of strain rate effects for UHPC in tension, Constr. Build. Mater. 153 (2017) 846–856.